Communications in Theoretical Physics

Commun. Theor. Phys. **77** (2025) 035004 (20pp) https://doi.org/10.1088/1572-9494/ad88f7

New dynamics performance for established dark solitons in polariton condensate

Emad H M Zahran[1], **Ahmet Bekir**[2] **and Reda A Ibrahim**[3]

[1] Department of Basic Science, Benha University, Faculty of Engineering, Shubra, Egypt
[2] Neighbourhood of Akcaglan, Imarli Street, Number: 28/4, 26030, Eskisehir, Turkey

E-mail: e_h_zahran@hotmail.com, bekirahmet@gmail.com and reda.mohamed@feng.bu.edu.eg

Received 13 June 2024, revised 19 October 2024
Accepted for publication 21 October 2024
Published 16 December 2024

Abstract

New diverse enormous soliton solutions to the Gross–Pitaevskii equation, which describes the dynamics of two dark solitons in a polarization condensate under non-resonant pumping, have been constructed for the first time by using two different schemes. The two schemes utilized are the generalized Kudryashov scheme and the (G'/G)-expansion scheme. Throughout these two suggested schemes we construct new diverse forms solutions that include dark, bright-shaped soliton solutions, combined bright-shaped, dark-shaped soliton solutions, hyperbolic function soliton solutions, singular-shaped soliton solutions and other rational soliton solutions. The two 2D and 3D figure designs have been configured using the Mathematica program. In addition, the Haar wavelet numerical scheme has been applied to construct the identical numerical behavior for all soliton solutions achieved by the two suggested schemes to show the existing similarity between the soliton solutions and numerical solutions.

Keywords: Gross–Pitaevskii equation, generalized Kudryashov schema, (G'/G)-technique, soliton solutions, numerical solutions

Gross–Pitaevskii equation	GPE
Generalized Kudryashov scheme	GKS
Haar Wavelet Numerical scheme	HWNS

1. Introduction

Generally, according to the soliton theory, the soliton is a solitary wave that has constant shape and speed that can be realized by cancelation of the nonlinear effect and the dispersion effect [1–5], for example, the static and dynamic characteristics of polarization Bose–Einstein condensates. This can be done through experimental studies of coherent nonlinear dynamics [6–11] in which these properties can be represented by the Gross–Pitaevskii equation, which is one of the forms of the nonlinear Schrodinger equation. The study of the soliton in polarization condensates is among the hottest topics and aims to obtain novel scenarios in which the combined effects of dissipation and nonlinearity on the nonlinear phenomena will disappear with an emphasis on capturing the non-equilibrium nature of the soliton with no analog in the static counterpart [12–21]. A number of dark solitons created by non-resonantly pumped excitation in a polarization condensate appear as the result of a moving defect that is dependent on the pump power [16]. The dynamics of two dark solitons in a polarization condensate under non-resonant pumping that can be described by the Gross–Pitaevskii equations coupled to the rate equation was first investigated theoretically [22]. The exaction polarization Bose–Einstein condensate in semiconductor micro cavities has been considered a novel platform to date, and has been the focus of major studies in nonlinear physics [23–26]. In this field of study, there are recent articles that discuss other nonlinear problems arising in various branches of physics, see, for example, Tariq *et al* [27] who applied three analytical approaches, namely the new extended hyperbolic function method, the modified extended tan hyperbolic function method and the new (G'/G^2)-expansion method, to derive a

* Author to whom any correspondence should be addressed.

variety of new multi-soliton solutions structures, in the form of dark, multi-bell shaped, singular bell shaped, trigonometric, hyperbolic and rational functions, to the coupled nonlinear (1+1)-dimensional Drinfel'd–Sokolov–Wilson equation in dispersive water waves, which is used to describe a nonlinear surface gravity wave propagating over a horizontal sea bed. Tariq *et al* [28] employed the extended modified auxiliary equation mapping approach and the (G'/G^2)-expansion method to study the Sharma–Tasso–Olver model. which characterizes the dynamical propagation of nonlinear double-dispersive evolution dispersive waves in heterogeneous mediums, and found that the model supports nonlinear solitary waves, periodic waves, shock waves and stable oscillatory waves. Using a set of appropriate parameters, Badshah *et al* [29] studied the anticipation of a bilinear Korteweg–De Vries (KdV) model known as the (1+1)-dimensional integro-differential Ito equation, which depicts oceanic shallow water wave dynamics using the (G'/G^2)-expansion approach, and the Adomian technique to acquire a variety of novel configurations for the governing dynamical model and established a collection of options for bright, dark, periodic, rational, and elliptic functions. Badshah *et al* [30] obtained some traveling and semi-analytical solitons to the extended (2+1)-dimensional Boussinesq model, which describes the propagation of waves with small amplitudes in shallow water propagating at a constant speed through a uniformly deep water canal using the Hirota bilinear technique, and established the bilinear structure of the governing equation. Ay and Yaşar [31], who studied the (2+1)-dimensional Chaffee–Infante equation, which occurs in the fields of fluid dynamics, high-energy physics, electronic science etc, built the Bäcklund transformations and residual symmetries in nonlocal structure using the Painlevé truncated expansion approach, delivered new exact solution profiles via the combination of various simple exact solution structures and acquired an infinite amount of exact solution forms methodically. The exaction–polarizations have a finite lifetime as the result of the imperfect confinement of the photon component, and they must be continuously re-populated and, hence, they lie between equilibrium Bose–Einstein condensates and lasers. We are interested in the Bose–Einstein condensates due to the non-resonant pumping created in a wire-shaped micro cavity similar to [32, 33], which bounds the polarities to a similar-dimensional channel. The condensate order parameter function $\psi(x,\ t)$ denotes, from the point of view of mean field theory, the driven-dissipative GPE connected by the density $nR(x,\ t)$ of reservoir polarizations [22] as follows:

$$\begin{aligned} \mathrm{i}\,\hbar\Psi_\tau &= \frac{-\hbar^2}{2m}\Psi_{xx} + g_R n_R \Psi \\ &\quad + \frac{\mathrm{i}\,\hbar}{2}(Rn_R - \gamma_c)\Psi + g_c(|\Psi|^2\Psi), \\ (n_R)_\tau &= P - (\gamma_R + R\,|\Psi|^2)n_R, \end{aligned} \tag{1}$$

where m is the relativistic mass of inferior polarizations; P is the level of an off-resonant continuous-wave thrusting; γ_c and γ_R describe the lifespan of the condensate and tank polarizations, respectively; R is the wave rate of scattering process of reservoir polarizations into the condensate; and g_c and g_R describe, respectively, the interaction coupling of the nonlinear interaction strength of polarizations and the interaction strength between reservoir and polarization. Note that the parameters g_c, g_R and R have been rescaled into the one-dimensional case by the width d of the nanowire thickness such that $g_c \to \frac{g_c}{\sqrt{2\pi d}}$, $g_R \to \frac{g_R}{\sqrt{2\pi d}}$, $R \to \frac{R}{\sqrt{2\pi d}}$.

By differentiating the first part of equation (1) with respect to the time we get

$$\begin{aligned} \mathrm{i}\hbar\Psi_{\tau\tau} &= \frac{-\hbar^2}{2m}\Psi_{xx\tau} + g_R n_R \Psi_\tau + g_R \Psi(n_R)_\tau \\ &\quad + \frac{\mathrm{i}\hbar}{2}(Rn_R - \gamma_c)\Psi_\tau + \frac{\mathrm{i}\hbar R}{2}(n_R)_\tau \Psi \\ &\quad + g_c(|\Psi|^2)_\tau \Psi + g_c\,|\Psi|^2(\Psi)_\tau. \end{aligned} \tag{2}$$

When the second part of equation (1) is substituted into equation (2) we get

$$\begin{aligned} &\frac{\hbar^2}{2m}\Psi_{xx\tau} + \mathrm{i}\hbar\Psi_{\tau\tau} - g_R n_R \Psi_\tau \\ &- g_R \Psi(P - n_R\gamma_R - n_R R\,|\Psi|^2) \\ &\quad - \frac{\mathrm{i}\hbar}{2}(Rn_R - \gamma_c)\Psi_\tau \\ &- \frac{\mathrm{i}\hbar R}{2}(P - (\gamma_R + R\,|\Psi|^2)n_R)\Psi \\ &- g_c(|\Psi|^2)_\tau \Psi - g_c\,|\Psi|^2\Psi_\tau = 0. \end{aligned} \tag{3}$$

Let us now consider the complex transformation

$$\begin{aligned} \Psi(x,\ \tau) &= u(\zeta)\mathrm{e}^{i\eta(x,\tau)}, \\ \zeta &= k\ x + w\ \tau, \\ \eta &= qx + \delta\tau + \vartheta_0, \end{aligned} \tag{4}$$

where $u(\eta)$ is the wave amplitude, while η denotes the phase amplitude, where k, ϑ_0, w are, respectively, frequency, phase constant and wave number. Simply from equation (4), we can construct the following relations

$$\Psi_x = (ku' + \mathrm{i}\ qu)\mathrm{e}^{\mathrm{i}\eta(x,\tau)}, \tag{5}$$

$$\Psi_{xx} = (-q^2u + 2\mathrm{i}kqu' + k^2u'')\mathrm{e}^{\mathrm{i}\eta(x,\tau)}, \tag{6}$$

$$\begin{aligned} \Psi_{xx\tau} &= -wq^2u' - \mathrm{i}\delta q^2 u + 2\mathrm{i}kqwu'' \\ &\quad - 2\delta qku' + k^2wu''' + \mathrm{i}\delta k^2u''\mathrm{e}^{\mathrm{i}\eta(x,\tau)}, \end{aligned} \tag{7}$$

$$\Psi_\tau = (wu' + \mathrm{i}\ \delta u)\mathrm{e}^{\mathrm{i}\eta(x,\tau)}, \tag{8}$$

$$\Psi_{\tau\tau} = (-\delta^2 u + 2\mathrm{i}\delta wu' + w^2u'')\mathrm{e}^{\mathrm{i}\eta(x,\tau)}, \tag{9}$$

$$|\Psi|^2 = u^2. \tag{10}$$

When the relations (5)–(10) are substituted into equation (3), which is dimensionless and $\hbar = m = 1$, and the real and imaginary terms separated, we get

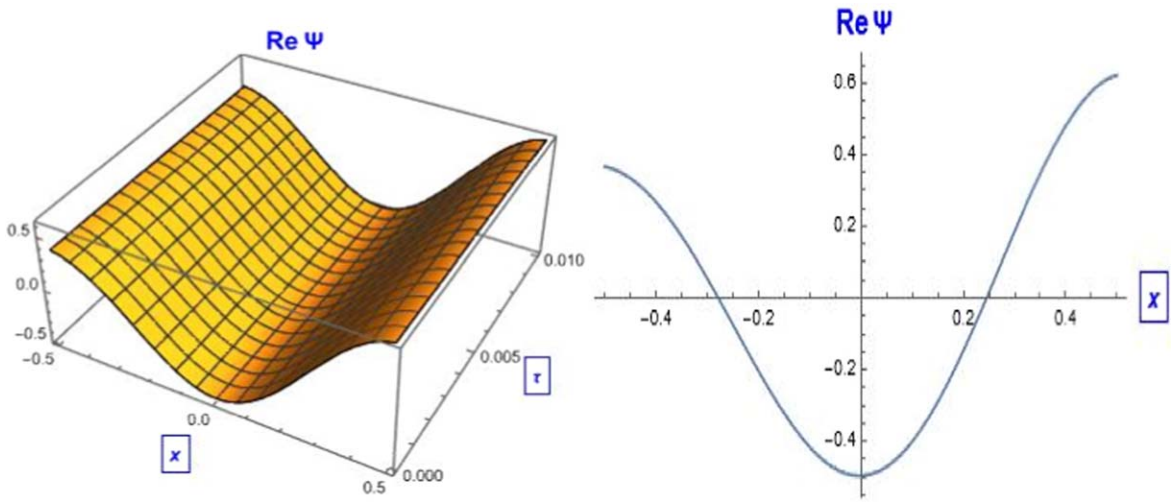

Figure 1. The 2D and 3D soliton solution behavior of equation (23) with the values given in equation (20).

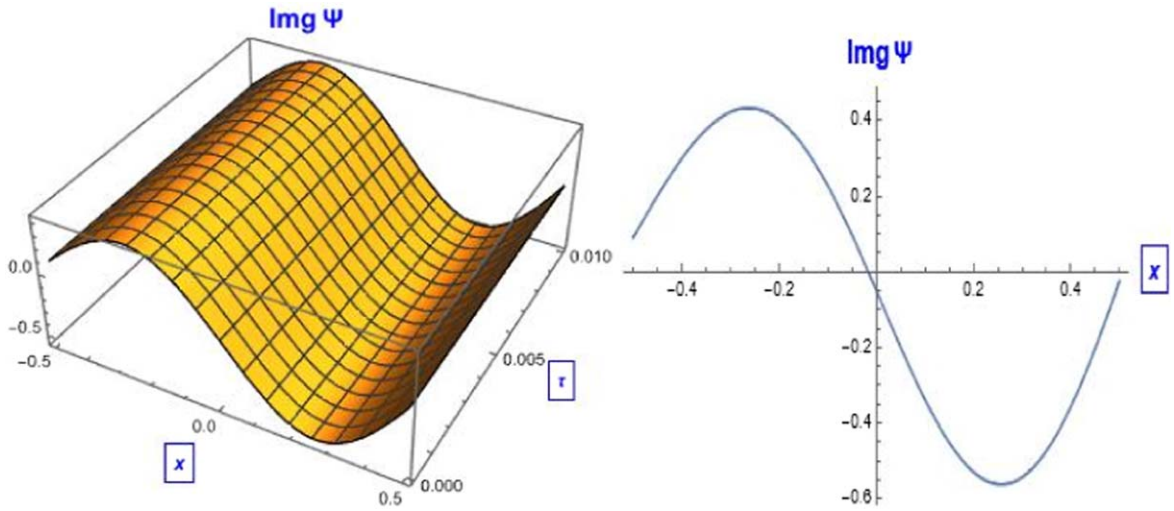

Figure 2. The 2D and 3D soliton solution behavior of equation (24) with the values given in equation (20).

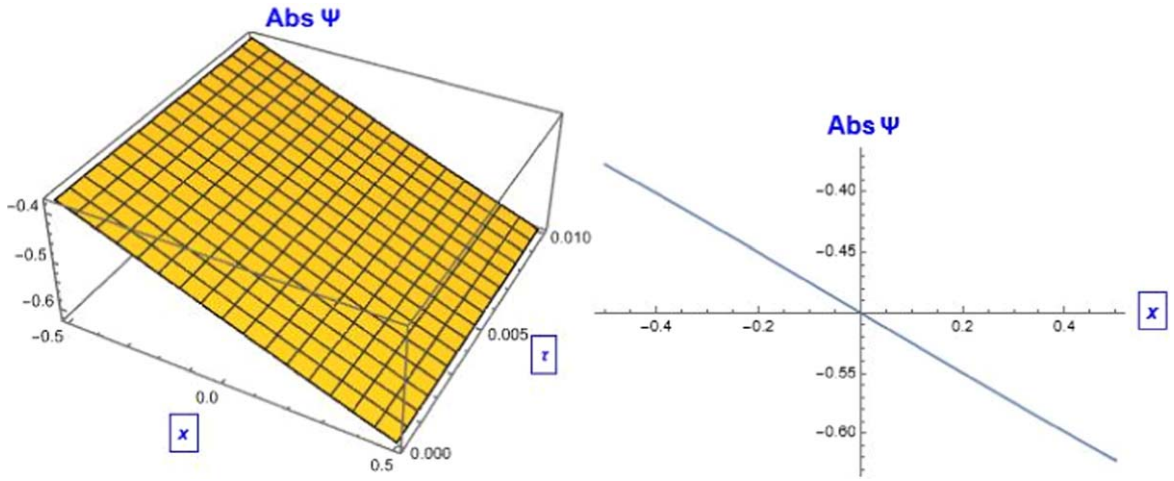

Figure 3. The 2D and 3D soliton solution behavior of $|\Psi|$.

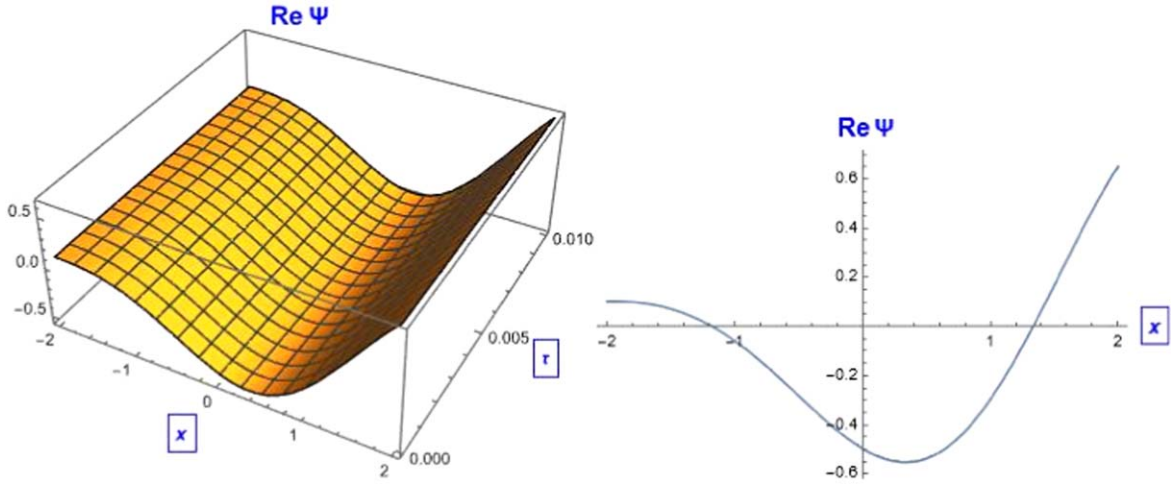

Figure 4. The 2D and 3D soliton solution behavior of equation (30) with the values given in equation (27).

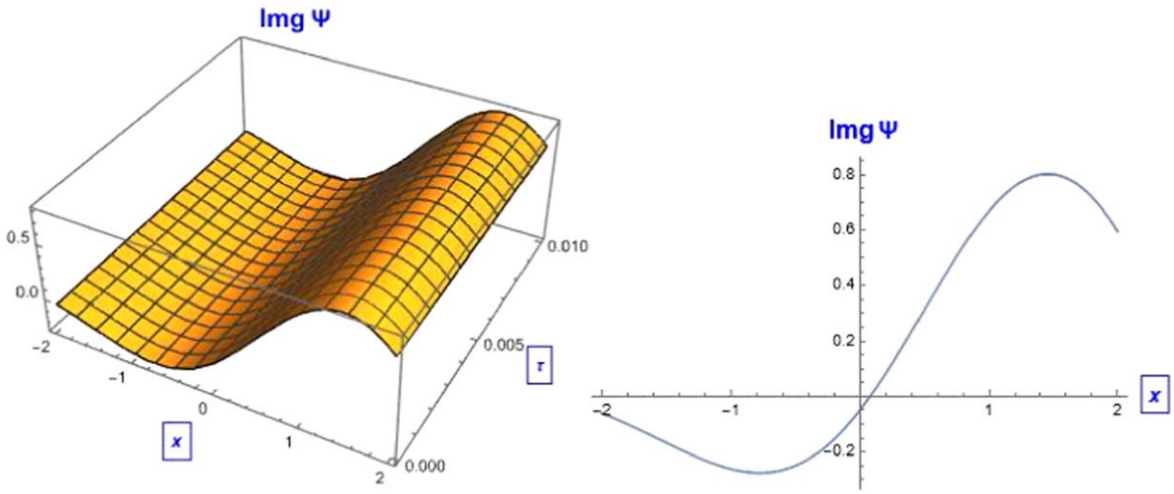

Figure 5. The 2D and 3D soliton solution behavior of equation (31) with the values given in equation (27).

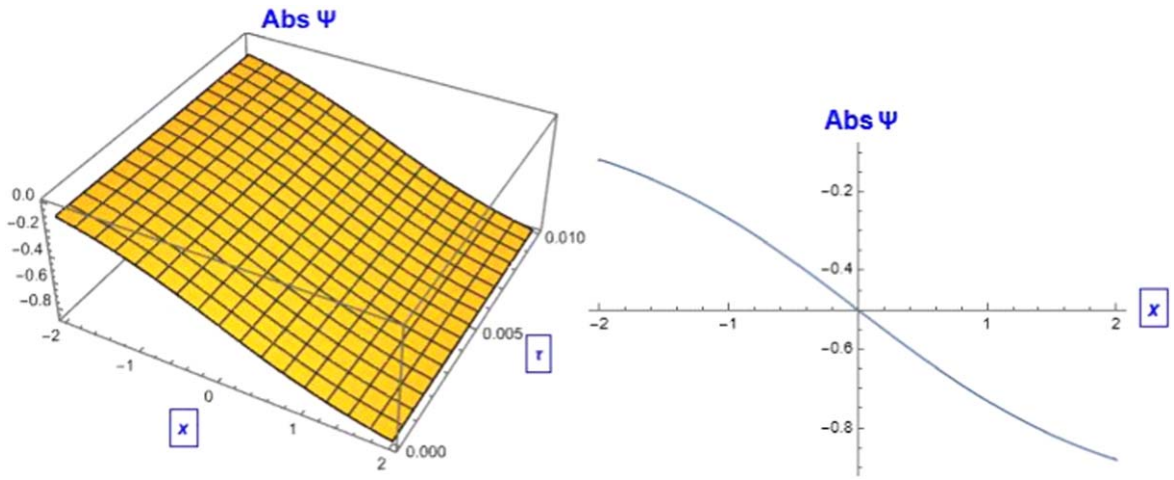

Figure 6. The 2D and 3D soliton solution behavior of $|\Psi|$.

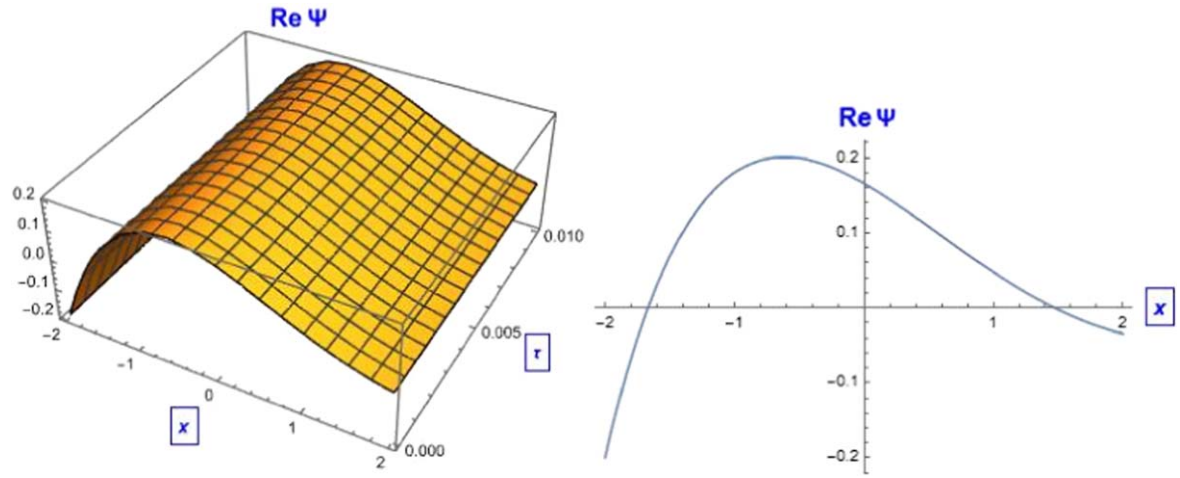

Figure 7. The soliton solution behaviors of equation (42) with the values given in equation (38) and $l_1 = 1$, $l_2 = 2$.

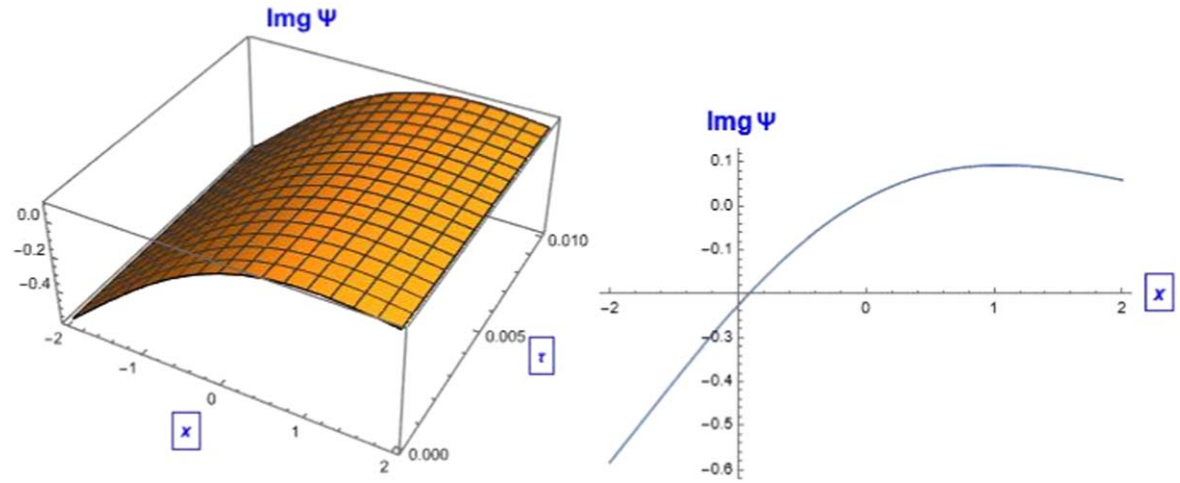

Figure 8. The soliton behavior of equation (43) with the values given in equation (38) and $l_1 = 1$, $l_2 = 2$.

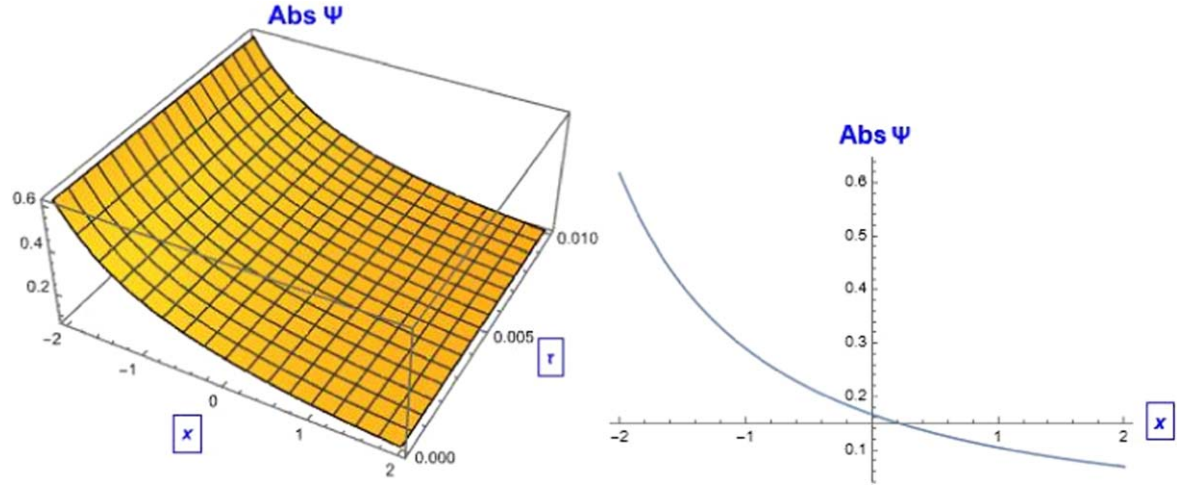

Figure 9. The 2D and 3D soliton solution behavior of $|\Psi|$.

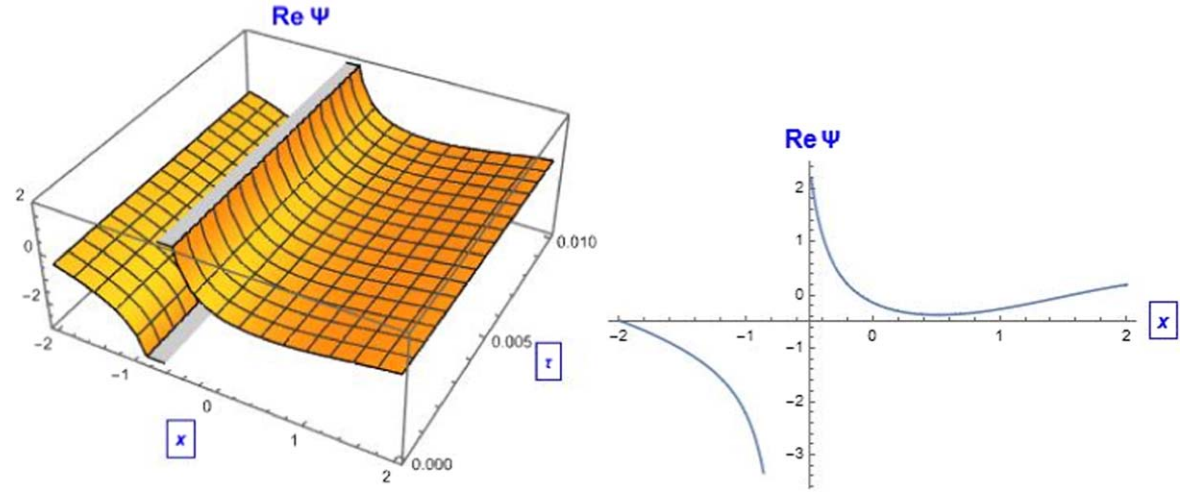

Figure 10. The soliton behavior of the Real (Re.) part of equation (49) with the values given in equation (46) and $l_1 = 1$, $l_2 = 2$.

$$\frac{k^2 w}{2}u''' - \left(\frac{1}{2}[wq^2 + 2\delta qk] + 2\delta w + g_R n_R w\right)u' + \left(g_R(\gamma_R n_R - P) - \frac{\delta}{2}(\gamma_c - Rn_R)\right)u - 3g_c w u^2 u' + Rg_R n_R u^3 = 0, \tag{11}$$

$$\left(\frac{k^2\delta}{2} + kqw + w^2\right)u'' + \left(\frac{R^2 n_R}{2} - \delta g_c\right)u^3 + \left(\frac{\gamma_c w}{2} - \frac{Rn_R w}{2}\right)u' - \left(\frac{q^2\delta}{2} + \delta^2 + g_R n_R \delta - \frac{R\gamma_R n_R}{2} + \frac{Rp}{2}\right)u = 0. \tag{12}$$

Throughout this study we will use the GKNS [34–37] and the $\left(\frac{G'}{G}\right)$-expansion scheme [38–40] to extract new soliton concepts for the proposed model that have not been described before.

2. The GKT-concept

To discuss the Generalized Kudryashov Technique (GKT) concept, we will investigate the formalism of the nonlinear partial differential equation (NLPDE) by supposing the function E of $u(x, \tau)$ and its partial derivatives as

$$E(u, u_x, u_\tau, u_{xx}, u_{\tau\tau},\ldots) = 0. \tag{13}$$

When we apply the transformation $u(x, \tau) = u(\zeta)$, $\zeta = kx + w\tau$, where k, ω are, respectively, the wave number and traveling wave speed to equation (13), it will be replaced by the following ordinary differential equation

$$R(u', u'', u''',\ldots) = 0, \tag{14}$$

in which R is a function of $u(x, \tau)$ and its total derivatives. The proposed solution of equation (14) according to the GKM is

$$u(\zeta) = \frac{\sum_{i=0}^{N} a_i P^i(\zeta)}{\sum_{j=0}^{M} b_j P^j(\zeta)} = \frac{a_0 + a_1 P(\zeta) + a_2 P^2(\zeta) + \ldots}{b_0 + b_1 P(\zeta) + b_2 P^2(\zeta) + \ldots}, \tag{15}$$

where the parameters a_i, $(i = 0, 1, 2, \ldots, N)$ and b_j, $(j = 0, 1, 2, \ldots, M)$ will be determined later such that $a_N \neq 0$, $b_M \neq 0$, while the function $P(\zeta)$ is the solution of the second-order nonlinear equation. The solution for the real part with balance number $M = 1$ is

$$\frac{\mathrm{d}P(\zeta)}{\mathrm{d}\zeta} = P^2(\zeta) - P(\zeta). \tag{16}$$

By integrating equation (16) we get

$$P(\zeta) = \frac{1}{1 + C\mathrm{e}^{\zeta}}. \tag{17}$$

Here, C is the integration constant. We will implement this method to the real part and the imaginary part individually.

2.1. For the real part

When one applies the balance rule between u''', u^2u' appears at equation (11) he will obtain $M = 1$, $\Rightarrow N = 2$; thus, the solution is

$$u(\zeta) = \frac{a_0 + a_1 P(\zeta) + a_2 P^2(\zeta)}{b_0 + b_1 P(\zeta)}. \tag{18}$$

By inserting u''', u^2u', u, u^3 into equation (11), setting the coefficients of various powers of $P^i(\zeta)$ equal to zero, a system of equations for the required unknown parameters will be explored from which we get 24 diverse enormous results; for similarity and simplicity, we will choose one of these results, which is

$$\begin{gathered} w \rightarrow -\frac{Rg_Rn_R}{3g_c},\ a_0 \rightarrow 0,\ b_0 \rightarrow 0, \\ \gamma_c \rightarrow \frac{-2Pg_cg_R + R\delta g_cn_R + 2k^2Rg_Rn_R + 2g_cg_Rn_R\gamma_R}{\delta g_c}, \\ \rightarrow \frac{3k\delta g_c + \sqrt{9k^2\delta^2g_c^2 + 7k^2R^2g_R^2n_R^2 - 4R^2\delta g_R^2n_R^2 - 2R^2g_R^3n_R^3}}{Rg_Rn_R}, \\ a_1 \rightarrow -a_2,\ b_1 \rightarrow \frac{a_2\sqrt{g_c}}{k}. \end{gathered} \tag{19}$$

Let us now design the 2D and 3D graphs of this solution that can be simplified to

$$\begin{gathered} C = \delta = R = g_c = g_R = \gamma_R = n_R = k = P = a_2 = 1, \\ a_0 = 0,\ a_1 = -1,\ b_0 = 0,\ b_1 = 1, \\ w = -0.3,\ \gamma_c = 3,\ q = 3 + \sqrt{10}. \end{gathered} \tag{20}$$

The solution according to these parameter values is

$$u(\zeta) = \frac{-e^{\zeta}}{e^{\zeta} + 1}, \tag{21}$$

$$\Psi(x, \tau) = \left(\frac{-e^{\left(x-\frac{1}{3}\tau\right)}}{e^{\left(x-\frac{1}{3}\tau\right)} + 1}\right)e^{i(6x+\tau+0.1)}, \tag{22}$$

$$\mathrm{Re}\,\Psi(x, \tau) = \left(\frac{-e^{\left(x-\frac{1}{3}\tau\right)}}{e^{\left(x-\frac{1}{3}\tau\right)} + 1}\right)\cos(6x + \tau + 0.1), \tag{23}$$

$$\mathrm{Im}\Psi(x, \tau) = \left(\frac{-e^{\left(x-\frac{1}{3}\tau\right)}}{e^{\left(x-\frac{1}{3}\tau\right)} + 1}\right)\sin(6x + \tau + 0.1). \tag{24}$$

2.2. For the imaginary part

When one applies the balance rule between u'', u^3 appears at equation (12) he will obtain $M = 1$; thus, the solution is

$$u(\zeta) = \frac{a_0 + a_1P(\zeta) + a_2P^2(\zeta)}{b_0 + b_1P(\zeta)}. \tag{25}$$

By inserting u'', u^3, u', u into equation (12), setting the coefficients of various powers of $P^i(\zeta)$ equal to zero, a system of equations for the required unknown parameters will be explored, from which we get 14 diverse enormous results; for similarity and simplicity, we will choose one of them, which is

$$\begin{gathered} a_0 \rightarrow 0,\ b_0 \rightarrow 0,\ \gamma_c \rightarrow \frac{-6\delta a_2^2g_c + 3R^2a_2^2n_R + 2Rwb_1^2n_R}{2wb_1^2}, \\ q \rightarrow \frac{-4w^2b_1^2 - 2k^2\delta b_1^2 + 2\delta a_2^2g_c - R^2a_2^2n_R}{4kwb_1^2}, \\ P \rightarrow \frac{\left\{\begin{array}{c} -16w^4\delta b_1^4 - 48k^2w^2\delta^2b_1^4 - 4k^4\delta^3b_1^4 - 32k^2w^2\delta a_2^2b_1^2g_c + 16w^2\delta^2a_2^2b_1^2g_c \\ +8k^2\delta^3a_2^2b_1^2g_c - 4\delta^3a_2^4g_c^2 + 16k^2R^2w^2a_2^2b_1^2n_R - 8R^2w^2\delta a_2^2b_1^2n_R - 4k^2R^2\delta^2a_2^2b_1^2n_R \\ +4R^2\delta^2a_2^4g_cn_R - 32k^2w^2\delta b_1^4g_Rn_R - R^4\delta a_2^4n_R^2 + 16k^2Rw^2b_1^4n_R\gamma_R \end{array}\right\}}{16k^2Rw^2b_1^4}, \\ a_1 \rightarrow -a_2. \end{gathered} \tag{26}$$

Let us now design the 2D and 3D graphs of the chosen result that can be simplified to

$$\begin{gathered} \delta = R = w = n_R = g_c = a_2 = b_1 = \gamma_R = k = g_R = 1, \\ a_0 = b_0 = 0,\ a_1 = -1,\ \gamma_c = -\frac{1}{2},\ P = -\frac{89}{16},\ q = -\frac{5}{4}. \end{gathered} \tag{27}$$

The solution according to these parameter values is

$$u(\zeta) = \frac{-e^{\zeta}}{e^{\zeta}+1}, \tag{28}$$

$$\Psi(x,\tau) = \left(\frac{-e^{(x+\tau)}}{e^{x+\tau}+1}\right)e^{i\left(\frac{-5}{4}x+\tau+0.1\right)}, \tag{29}$$

$$\mathrm{Re}\,\Psi(x,\tau) = \left(\frac{-e^{(x+\tau)}}{e^{(x+\tau)}+1}\right)\cos\left(\frac{-5}{4}x+\tau+0.1\right), \tag{30}$$

$$\mathrm{Im}\Psi(x,\tau) = \left(\frac{-e^{(x+\tau)}}{e^{(x+\tau)}+1}\right)\sin\left(\frac{-5}{4}x+\tau+0.1\right). \tag{31}$$

3. The (G'/G)-expansion scheme

This scheme proposes the solution of equation (14) to be in the form

$$u(\eta) = A_0 + \sum_{i=1}^{M} A_i\left[\frac{G'}{G}\right]^i, A_M \neq 0, \tag{32}$$

where M is the balance number. The function $G(\zeta)$ achieves the second-order differential equation $G'' + \mu G' + \lambda G = 0$ that has three types of solution depending on the discriminate of this equation, which has one of these cases:

(I) If $\mu^2 - 4\lambda \succ 0$, then the solution is

$$\left(\frac{G'}{G}\right) = \frac{\sqrt{\mu^2-4\lambda}}{2} \times \left(\frac{l_1 \sinh\left(\frac{\sqrt{\mu^2-4\lambda}}{2}\right)\zeta + l_2 \cosh\left(\frac{\sqrt{\mu^2-4\lambda}}{2}\right)\zeta}{l_1 \cosh\left(\frac{\sqrt{\mu^2-4\lambda}}{2}\right)\zeta + l_2 \sinh\left(\frac{\sqrt{\mu^2-4\lambda}}{2}\right)\zeta}\right) - \frac{\mu}{2}. \tag{33}$$

(II) If $\mu^2 - 4\lambda \prec 0$, then the solution is

$$\left(\frac{G'}{G}\right) = \frac{\sqrt{\mu^2-4\lambda}}{2} \times \left(\frac{-l_1 \sin\left(\frac{\sqrt{\mu^2-4\lambda}}{2}\right)\zeta + l_2 \cos\left(\frac{\sqrt{\mu^2-4\lambda}}{2}\right)\zeta}{l_1 \cos\left(\frac{\sqrt{\mu^2-4\lambda}}{2}\right)\zeta + l_2 \sin\left(\frac{\sqrt{\mu^2-4\lambda}}{2}\right)\zeta}\right) - \frac{\mu}{2}. \tag{34}$$

(III) If $\mu^2 - 4\lambda = 0$, then the solution is

$$\left(\frac{G'}{G}\right) = \left(\frac{l_2}{l_1 + l_2\zeta}\right) - \frac{\mu}{2}. \tag{35}$$

Let us now apply this concept for the above real part and imaginary part of equations (11) and (12), respectively.

3.1. Solution for the real part with balance number $M = 1$

$$u(\zeta) = A_0 + A_1\left(\frac{G'}{G}\right). \tag{36}$$

By computing u''', u^2u', u, u^3 and inserting in equation (11), setting the coefficients of various powers of $\left(\frac{G'}{G}\right)^i$ equal to zero, a system of equations for the required unknown parameters will be explored, from which we get unique result, which is

$$\lambda \to \frac{A_0(3k^2wA_0 + RA_1^3 g_R n_R)}{3k^2wA_1^2},$$

$$\mu \to \frac{6k^2wA_0 + RA_1^3 g_R n_R}{3k^2wA_1},$$

$$\delta \to \frac{-9k^2q^2w^2 - 18k^2w^2 g_R n_R + 7R^2A_1^4 g_R^2 n_R^2}{18k^2w(kq+2w)},$$

$$\gamma_c \to \left(\frac{\begin{array}{c}36k^5Pqw^2g_R + 72k^4Pw^3g_R + 9k^4q^2Rw^3n_R + 18k^4Rw^3g_R n_R^2 - 7k^2R^3wA_1^4 g_R^2 n_R^3 \\ -4kqR^3A_1^6 g_R^3 n_R^3 - 8R^3wA_1^6 g_R^3 n_R^3 - 36k^5qw^2g_R n_R\gamma_R - 72k^4w^3g_R n_R\gamma\end{array}}{k^2w(9k^2q^2w^2 + 18k^2w^2g_R n_R - 7R^2A_1^4 g_R^2 n_R^2)}\right),$$

$$g_c \to \frac{k^2}{A_1^2}. \tag{37}$$

This result can be streamlined to the following values

$$\begin{aligned} &g_R = k = R = A_1 = w = \gamma_R \\ &\quad = A_0 = P = q = n_R = g_c = 1, \\ &\lambda = \frac{4}{3},\ \mu = \frac{7}{3},\ \gamma_c = \frac{2}{5},\ \delta \to -\frac{10}{27}, \end{aligned} \tag{38}$$

from which we have $\mu^2 - 4\lambda = \frac{1}{9} \succ 0$, which implies the form equation (11) for $\left(\frac{G'}{G}\right)$ cases is

$$\left(\frac{G'}{G}\right) = \frac{1}{6}\left(\frac{l_1 \sin h\left(\frac{1}{6}\right)\zeta + l_2 \cos h\left(\frac{1}{6}\right)\zeta}{l_1 \cos h\left(\frac{1}{6}\right)\zeta + l_2 \sin h\left(\frac{1}{6}\right)\zeta}\right) - \frac{7}{6}, \tag{39}$$

Let us now design the 2D and 3D graphs of equations (42) and (43)

3.2. The (G'/G)-expansion scheme for the imaginary part

As we noted before, the balance number for imaginary part equation (12) is $M = 1$; hence, the solution is

$$u(\zeta) = A_0 + A_1\left(\frac{G'}{G}\right). \tag{44}$$

By computing u'', u', u, u^3 and inserting in equation (12), setting the coefficients of various powers of $\left(\frac{G'}{G}\right)^i$ equal to zero, a system of equations for the required unknown parameters will be explored, from which we get three different results; for simplicity we choose the first one, which is

$$\begin{aligned} \lambda \to &\frac{4kqwA_0^2 + 4w^2A_0^2 + 2k^2\delta A_0^2 + PRA_1^2 + q^2\delta A_1^2 + 2\delta^2 A_1^2 + 2\delta A_1^2 g_R n_R - RA_1^2 n_R \gamma_R}{2(2kqw + 2w^2 + k^2\delta)A_1^2}, \\ &\mu \to \frac{2A_0}{A_1},\ g_c \to \frac{4kqw + 4w^2 + 2k^2\delta + R^2A_1^2 n_R}{2\delta A_1^2},\ \gamma_c \to Rn_R. \end{aligned} \tag{45}$$

$$\begin{aligned} u(\zeta) &= 1 + \frac{1}{6}\left(\frac{l_1 \sin h\left(\frac{1}{6}\right)\zeta + l_2 \cos h\left(\frac{1}{6}\right)\zeta}{l_1 \cos h\left(\frac{1}{6}\right)\zeta + l_2 \sin h\left(\frac{1}{6}\right)\zeta}\right) - \frac{7}{6} \\ &= \frac{1}{6}\left(\frac{l_1 \sin h\left(\frac{1}{6}\right)\zeta + l_2 \cos h\left(\frac{1}{6}\right)\zeta}{l_1 \cosh\left(\frac{1}{6}\right)\zeta + l_2 \sinh\left(\frac{1}{6}\right)\zeta} - 1\right), \end{aligned} \tag{40}$$

$$\begin{aligned} \Psi(x,\tau) &= \frac{1}{6} \\ &\times \left(\frac{l_1 \sin h\left(\frac{1}{6}(x+\tau)\right) + l_2 \cos h\left(\frac{1}{6}(x+\tau)\right)}{l_1 \cos h\left(\frac{1}{6}(x+\tau)\right) + l_2 \sin h\left(\frac{1}{6}(x+\tau)\right)} - 1\right) \\ &\times e^{i\left(x - \frac{10}{27}\tau + 0.1\right)}, \end{aligned} \tag{41}$$

$$\begin{aligned} \mathrm{Re}\,\Psi(x,\tau) &= \frac{1}{6} \\ &\times \left(\frac{l_1 \sin h\left(\frac{1}{6}(x+\tau)\right) + l_2 \cos h\left(\frac{1}{6}(x+\tau)\right)}{l_1 \cos h\left(\frac{1}{6}(x+\tau)\right) + l_2 \sin h\left(\frac{1}{6}(x+\tau)\right)} - 1\right) \\ &\times \cos\left(x - \frac{10}{27}\tau + 0.1\right), \end{aligned} \tag{42}$$

$$\begin{aligned} \mathrm{Im}\Psi(x,\tau) &= \frac{1}{6} \\ &\times \left(\frac{l_1 \sin h\left(\frac{1}{6}(x+\tau)\right) + l_2 \cos h\left(\frac{1}{6}(x+\tau)\right)}{l_1 \cos h\left(\frac{1}{6}(x+\tau)\right) + l_2 \sin h\left(\frac{1}{6}(x+\tau)\right)} - 1\right) \\ &\times \sin\left(x - \frac{10}{27}\tau + 0.1\right). \end{aligned} \tag{43}$$

This result can be streamlined to be in the form

$$\begin{aligned} &g_R = k = R = A_1 = w = \gamma_R \\ &\quad = A_0 = P = q = \delta = n_R = \gamma_c = 1, \\ &\lambda = \frac{3}{2},\ \mu = 2,\ g_c = \frac{11}{2}, \end{aligned} \tag{46}$$

from which we have $\mu^2 - 4\lambda = -2 \prec 0$, so the solution from $\left(\frac{G'}{G}\right)$ point of view equation (12) is

$$u(\zeta) = \frac{i}{\sqrt{2}}\left(\frac{-l_1 \sin\left(\frac{i}{\sqrt{2}}\right)\zeta + l_2 \cos\left(\frac{i}{\sqrt{2}}\right)\zeta}{l_1 \cos\left(\frac{i}{\sqrt{2}}\right)\zeta + l_2 \sin\left(\frac{i}{\sqrt{2}}\right)\zeta}\right), \tag{47}$$

$$\begin{aligned} \Psi(x,\tau) &= \frac{i}{\sqrt{2}} \\ &\times \left(\frac{-l_1 \sin\left(\frac{i(x+\tau)}{\sqrt{2}}\right) + l_2 \cos\left(\frac{i(x+\tau)}{\sqrt{2}}\right)}{l_1 \cos\left(\frac{i(x+\tau)}{\sqrt{2}}\right) + l_2 \sin\left(\frac{i(x+\tau)}{\sqrt{2}}\right)}\right) \\ &\times e^{i(x+\tau+0.1)}, \end{aligned} \tag{48}$$

$$\begin{aligned} \mathrm{Re}\,\Psi(x,\tau) &= \frac{-i}{\sqrt{2}} \\ &\times \left(\frac{-l_1 \sin\left(\frac{i(x+\tau)}{\sqrt{2}}\right) + l_2 \cos\left(\frac{i(x+\tau)}{\sqrt{2}}\right)}{l_1 \cos\left(\frac{i(x+\tau)}{\sqrt{2}}\right) + l_2 \sin\left(\frac{i(x+\tau)}{\sqrt{2}}\right)}\right) \\ &\times \sin(x + \tau + 0.1), \end{aligned} \tag{49}$$

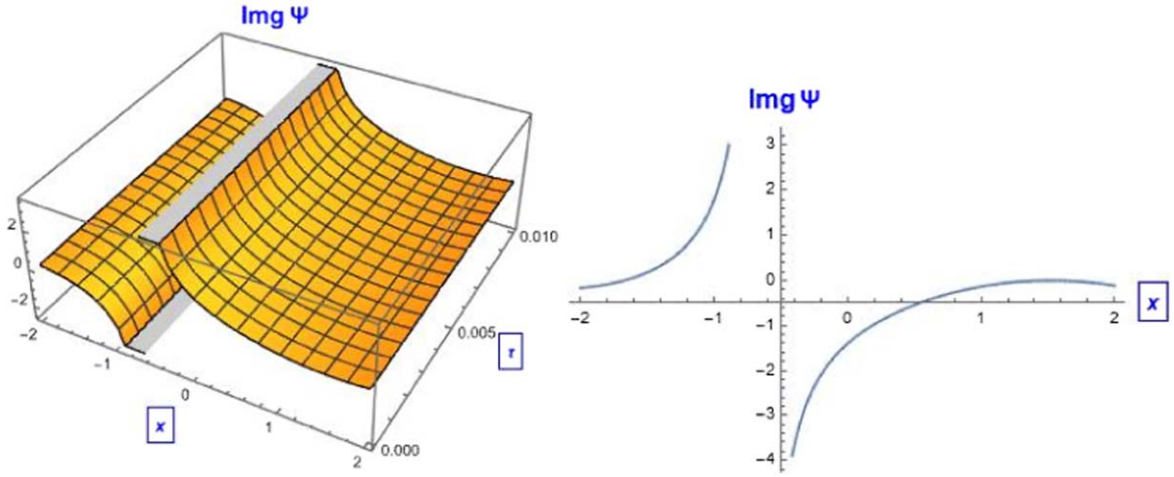

Figure 11. The soliton behavior of the Imaginary (Im.) part of equation (50) with the values given in equation (46) and $l_1 = 1$, $l_2 = 2$.

$$\mathrm{Im}\Psi(x,\tau) = \frac{\mathrm{i}}{\sqrt{2}} \times \left(\frac{-l_1 \sin\left(\frac{\mathrm{i}(x+\tau)}{\sqrt{2}}\right) + l_2 \cos\left(\frac{\mathrm{i}(x+\tau)}{\sqrt{2}}\right)}{l_1 \cos\left(\frac{\mathrm{i}(x+\tau)}{\sqrt{2}}\right) + l_2 \sin\left(\frac{\mathrm{i}(x+\tau)}{\sqrt{2}}\right)} \right) \times \cos(x+\tau+0.1). \tag{50}$$

4. The algorithm of HWNS

The wavelet is considered as one of the powerful and fast evolving methods to obtain a numerical solution of ordinary and partial differential equations with increasing applications in physics and engineering problems. The development of the Haar wavelet in the construction of the numerical solution started in 1997 when Chen and Hsiao [41] introduced an operational matrix of integration to solve the suggested models of dynamic systems. They suggested the notation of expressing the function corresponding to highest derivative of a differential equation as a Haar wavelet series. Lepik [42–44] introduced the Haar wavelet numerical scheme with a uniform grid for the solution of differential, integral, integro-differential and fractional integral equations. As a vital part of this work, we attempt to extend this method to examine the results for higher order nonlinear boundary value problems with semi-infinite or infinite domain, thus making the method more useful in real-world applications.

4.1. Haar wavelet functions and their integration

The Haar wavelet functions [45] are given as

$$h_i(t) = \begin{cases} 1; & for\ t \in [\nu_1, \nu_2] \\ -1; & for\ t \in [\nu_2, \nu_2]. \\ 0; & \text{otherwise} \end{cases} \tag{51}$$

This is considered as the simplest wavelet function in the structure of building basis functions because it uses only two operations, translation and dilation.

With $\nu_1 = \frac{k}{m}$, $\nu_2 = \frac{k+0.5}{m}$, $\nu_3 = \frac{k+1}{m}$: the integer number $m = 2^j$; $j = 0, 1, 2, \ldots, J$ indicates the level of the wavelet (dilation parameter); and $k = 0, 1, 2, \ldots, m-1$ is the translation parameter. The integer J is the maximal level of resolution; the index i is computed from $i = m + k + 1$, which has minimum value $i = 2(m = 1, k = 0)$, for which the Haar function is called the mother function, and maximum value $i = 2M$, $M = 2^J$ the index $i = 1$ corresponds to the scaling (father) function:

$$h_1(t) = \begin{cases} 1; & for\ 0 \leqslant t \prec 1 \\ 0; & elsewhere \end{cases}. \tag{52}$$

The following relations according to [41–45] are important to introduce

$$\begin{aligned} p_i(t) &= \int_0^t h_i(x)\mathrm{d}x; \\ Q_i(t) &= \int_0^t p_i(x)\mathrm{d}x; \\ R_i(t) &= \int_0^t Q_i(x)\mathrm{d}x. \end{aligned} \tag{53}$$

Integrating the Haar functions with respect to t from $0 \to x$, we can obtain the following important special relations:

$$p_i(t) = \begin{cases} t - \nu_1; & for\ t \in [\nu_1,\ \nu_2] \\ \nu_3 - t; & for\ t \in [\nu_2,\ \nu_3], \\ 0; & elsewhere \end{cases} \tag{54}$$

$$Q_i(t) = \begin{cases} 0; & for\ t \in [0, \nu_1] \\ \frac{(t-\nu_1)^2}{2}; & for\ t \in [\nu_1, \nu_2] \\ \frac{1}{4m^2} - \frac{(\nu_3 - t)^2}{2}; & for\ t \in [\nu_2, \nu_3] \\ \frac{1}{4m^2}; & for\ t \in [\nu_3, 1] \end{cases}, \tag{55}$$

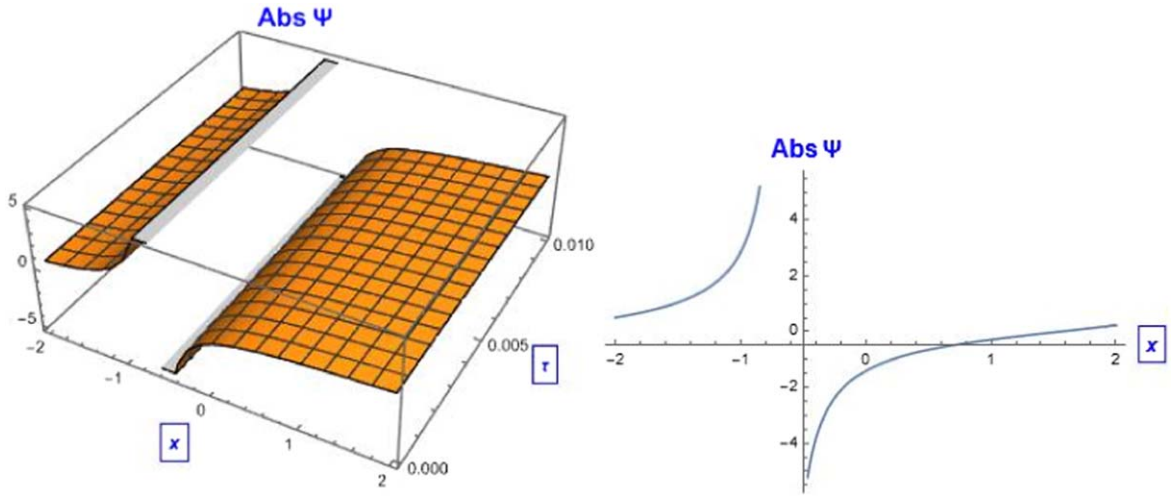

Figure 12. The 2D and 3D soliton solution behavior of $|\Psi|$.

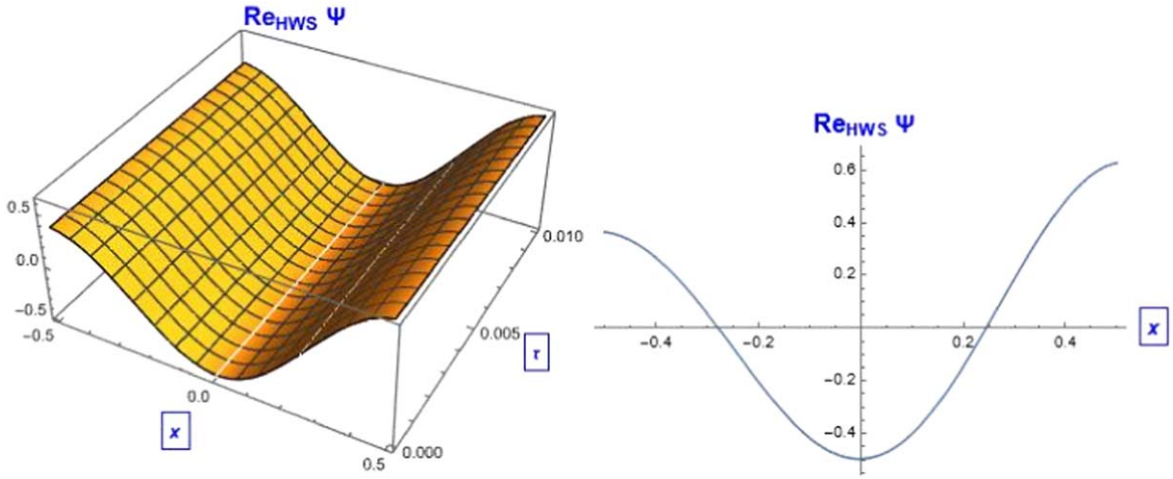

Figure 13. The HW numerical solution behavior of the Re. part of equation (73) with values given in equation (61).

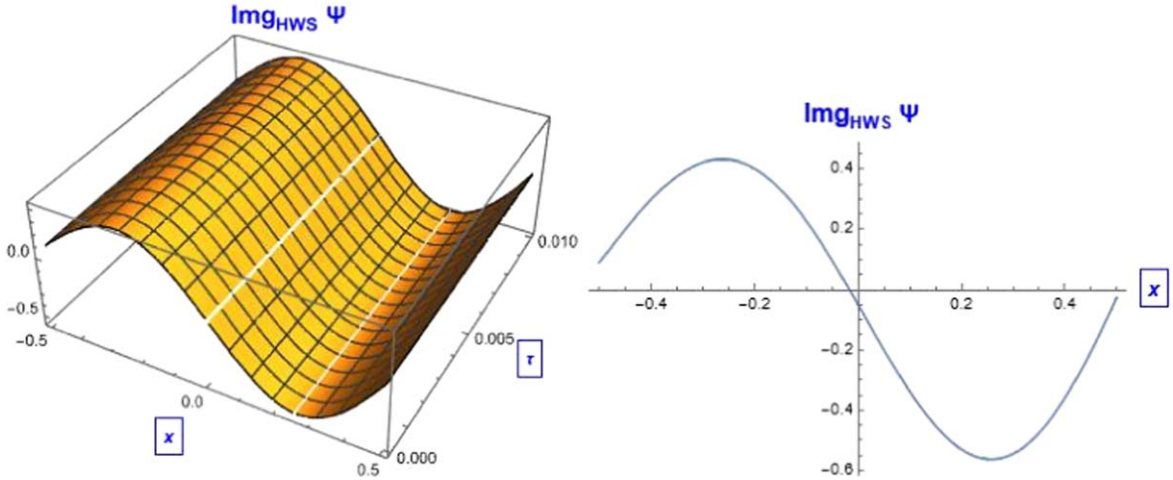

Figure 14. The HW numerical solution behavior to the Im. part of equation (74) with values given in equation (61).

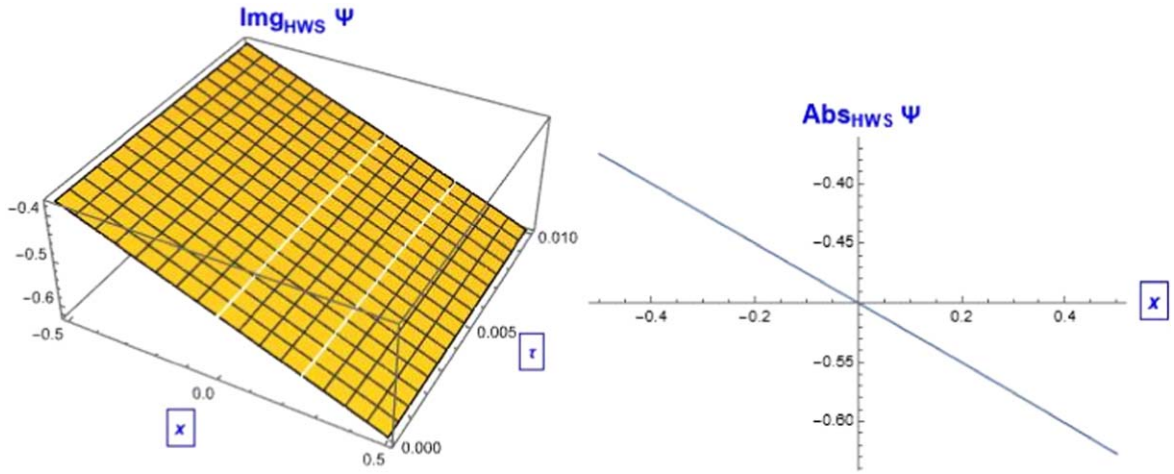

Figure 15. The 2D and 3D soliton HWN solution behavior of $|\Psi|$ equations (73) or (74).

$$R_i(t) = \begin{cases} 0; & for\ t \in [0,\ \nu_1] \\ \dfrac{(t-\nu_1)^3}{6}; & for\ t \in [\nu_1,\ \nu_2] \\ \dfrac{(t-\nu_2)}{4m^2} - \dfrac{(\nu_3 - t)^3}{6}; & for\ t \in [\nu_2,\ \nu_3] \\ \dfrac{t-\nu_2}{4m^2}; & for\ t \in [\nu_3,\ 1] \end{cases}. \quad (56)$$

4.2. Haar wavelet functions and collocation points [41–45]

Since the numerical solution is computed first at discrete points, in this case called collation points, to find the solution of the differential equation we discretize the equation in Haar functions $h_i(t)$ in the following manner.

Firstly, we will divide the interval $t \in [0,\ 1]$ into $2M$ parts of equal length $\Lambda(t) = \dfrac{1}{2M}$, then we compute the collocation points from

$$t_l = \frac{l - 0.5}{2M}. \quad (57)$$

Any function $\psi(t)$, $t \in [0,\ 1]$ can be written as

$$\psi(t) = \sum_{i=1}^{2M} a_i h_i(t) = a_1 h_1(t) + a_2 h_2(t) + \ \ldots + a_{2M} h_{2M}(t), \quad (58)$$

where α_i denotes the Haar coefficients. Multiplying equation (58) by $h_m(t)$, and integrating from $0 \to 1$, one obtains

$$\int_0^1 \psi(t) h_m(t) \mathrm{d}t = a_i \sum_{i=1}^{2M} \int_0^1 h_i(t) h_m(t) \mathrm{d}t.$$

And from the orthogonal property, we get the coefficients a_i

$$\int_0^1 h_i(t) h_m(t) \mathrm{d}t = \begin{cases} 2^{-j}; & if\ i = m \\ 0; & if\ i \neq m \end{cases} \Rightarrow \left[a_i = 2^j \int_0^1 \psi(t) h_m(t) \mathrm{d}t \right]. \quad (59)$$

Satisfying equation (58) at collocation points

$$\psi(t_l) = \sum_{i=1}^{2M} a_i h_i(t_l) = \sum_{i=1}^{2M} a_i X_{il}, \quad (60)$$

which can be written in matrix form $\Xi = aX$, where Ξ and a are $2M$ vectors and $X = X_{il} = h_i(t_l)$ are the coefficients matrix with dimension $(2M \times 2M)$.

4.3. The numerical solution using the HWNS corresponding to the exact solution derived by GKS (real part)

It is a vital aim in this work to construct the numerical solution corresponding to the analytical soliton solution obtained by GKS and the $\left(\dfrac{G'}{G}\right)$-expansion scheme to show the reliability of the obtained analytical soliton solutions.

Consider the real part of equation (11) with values

$$\delta = R = g_c = g_R = \gamma_R = n_R = k = P = 1,$$
$$w = \frac{-1}{3},\ \gamma_c = 3,\ q = 3 + \sqrt{10}. \quad (61)$$

This can be written as

$$\frac{1}{2} u'''(\zeta) + u'(\zeta) + u'(\zeta) u^2(\zeta) - u(\zeta) + u^3(\zeta) = 0, \quad (62)$$

whose exact solution derived by GKM is equation (21), which has the following initial conditions

$$u(0) = -\frac{1}{2},\ u'(0) = -\frac{1}{4},\ u''(0) = 0. \quad (63)$$

According to HWNS, the solution of equation (62) is put in the form

$$u'''(\zeta) = \sum_{i=1}^{2M} a_i h_i(\zeta). \quad (64)$$

By integrating equation (64) three times w.r.t. ζ from $0 \to \zeta$

to obtain $u(\zeta)$ we obtain

$$u''(\zeta) = \sum_{i=1}^{2M} a_i p_i(\zeta) + u''(0) = \sum_{i=1}^{2M} a_i p_i(\zeta), \tag{65}$$

$$\begin{aligned} u'(\zeta) &= \sum_{i=1}^{2M} a_i Q_i(\zeta) + u'(0) \\ &= -\frac{1}{4} + \sum_{i=1}^{2M} a_i Q_i(\zeta), \end{aligned} \tag{66}$$

$$\begin{aligned} u(\zeta) &= \sum_{i=1}^{2M} a_i R_i(\zeta) - \frac{1}{4}\zeta + u(0) \\ &= -\frac{1}{2} - \frac{1}{4}\zeta + \sum_{i=1}^{2M} a_i R_i(\zeta). \end{aligned} \tag{67}$$

Inserting equations (64)–(67) into equation (62) we obtain

$$\begin{aligned} &\frac{1}{2}\sum_{i=1}^{2M} a_i h_i(\zeta) \; - \frac{1}{4} + \sum_{i=1}^{2M} a_i Q_i(\zeta) \\ &+\left(-\frac{1}{4} + \sum_{i=1}^{2M} a_i Q_i(\zeta)\right)\left(-\frac{1}{2} - \frac{1}{4}\zeta + \sum_{i=1}^{2M} a_i R_i(\zeta)\right)^2 \\ &+ \frac{1}{2} + \frac{1}{4}\zeta - \sum_{i=1}^{2M} a_i R_i(\zeta) \\ &+\left(-\frac{1}{2} - \frac{1}{4}\zeta + \sum_{i=1}^{2M} a_i R_i(\zeta)\right)^3 = 0. \end{aligned} \tag{68}$$

When equation (68) surrenders to the collocation points given in equation (57) we get

$$\begin{aligned} &\frac{1}{2}\sum_{i=1}^{2M} a_i h_i(\zeta_l) - \frac{1}{4} + \sum_{i=1}^{2M} a_i Q_i(\zeta_l) \\ &+\left(-\frac{1}{4} + \sum_{i=1}^{2M} a_i Q_i(\zeta)\right)\left(-\frac{1}{2} - \frac{1}{4}\zeta_l + \sum_{i=1}^{2M} a_i R_i(\zeta_l)\right)^2 \\ &+ \frac{1}{2} + \frac{1}{4}\zeta_l - \sum_{i=1}^{2M} a_i R_i(\zeta_l) \\ &+\left(-\frac{1}{2} - \frac{1}{4}\zeta_l + \sum_{i=1}^{2M} a_i R_i(\zeta_l)\right)^3 = 0\,, \;\; l = 1, 2, \ldots, 2M. \end{aligned} \tag{69}$$

Putting the level of resolution $J = 1 \to M = 2^J = 2 \to 2M = 4 \to l = 1, 2, 3, 4$, then equation (69) becomes

$$\begin{aligned} &\frac{1}{2}\sum_{i=1}^{4} a_i h_i(\zeta_l) - \frac{1}{4} + \sum_{i=1}^{4} a_i Q_i(\zeta_l) \\ &+\left(-\frac{1}{4} + \sum_{i=1}^{4} a_i Q_i(\zeta)\right)\left(-\frac{1}{2} - \frac{1}{4}\zeta_l + \sum_{i=1}^{4} a_i R_i(\zeta_l)\right)^2 \\ &+ \frac{1}{2} + \frac{1}{4}\zeta_l - \sum_{i=1}^{4} a_i R_i(\zeta_l) \\ &+\left(-\frac{1}{2} - \frac{1}{4}\zeta_l + \sum_{i=1}^{4} a_i R_i(\zeta_l)\right)^3 = 0\,. \end{aligned} \tag{70}$$

Equation (70), at collocation points $\zeta_l = \dfrac{l - 0.5}{2M} = \dfrac{l - 0.5}{4}$, $l = 1, 2, 3, 4$, leads to a system of unknowns a_i, $i = 1, 2, 3, 4$, and by solving this system we get

$$\begin{aligned} a_1 &= -0.00279276, \\ a_2 &= -0.0929915, \\ a_3 &= -0.0262158, \\ a_4 &= -0.0656008. \end{aligned} \tag{71}$$

Using equation (71) in equation (67), then the Haar wavelet solution of equation (62) is

$$\begin{aligned} u(\zeta) &= -\frac{1}{2} - \frac{1}{4}\zeta + a_1 R_1(\zeta) + a_2 R_2(\zeta) \\ &+a_3 R_3(\zeta) + a_4 R_4(\zeta) = -\frac{1}{2} - \frac{1}{4}\zeta \\ &-0.00279276\, R_1(\zeta) - 0.0929915\, R_2(\zeta) \\ &-0.0262158\, R_3(\zeta) - 0.0656008\, R_4(\zeta). \end{aligned} \tag{72}$$

Hence,

$$\Psi(x, \tau) = u(\zeta) e^{i\eta(x,\tau)}$$

$$\begin{aligned} &\mathrm{Re}\,\Psi(x, \tau) = \\ &\left(\begin{array}{l} -0.5 - 0.25\left(x - \frac{1}{3}\tau\right) - 0.00279276 R_1\left[x - \frac{1}{3}\tau\right] \\ -0.0929915 R_2\left[x - \frac{1}{3}\tau\right] \\ -0.026216 R_3\left[x - \frac{1}{3}\tau\right] - 0.0656008 R_4\left[x - \frac{1}{3}\tau\right] \end{array}\right) \\ &\times \cos\left[6x + \tau + 0.1\right], \end{aligned} \tag{73}$$

$$\begin{aligned} &\mathrm{Im}\Psi(x, \tau) = \\ &\left(\begin{array}{c} -0.5 - 0.00279276 R_1\left[x - \frac{1}{3}\tau\right] \\ -0.0929915 R_2\left[x - \frac{1}{3}\tau\right] - 0.25\left(x - \frac{1}{3}\tau\right) \\ -0.02622 R_3\left[x - \frac{1}{3}\tau\right] - 0.065601 R_4\left[x - \frac{1}{3}\tau\right] \end{array}\right) \\ &\times \sin\left[6x + \tau + 0.1\right]. \end{aligned} \tag{74}$$

4.4. The numerical solution using the HWNS corresponding to the exact solution derived by GKS (imaginary part)

For the imaginary part equation (12) with the following

$$\begin{aligned} &\delta = R = g_c = g_R = \gamma_R = n_R = w = k = 1, \\ &P = \frac{-89}{16}, \gamma_c = -\frac{1}{2}, q = -\frac{5}{4}, \end{aligned} \tag{75}$$

becomes

$$\frac{1}{4}u''(\zeta) - \frac{3}{4}u'(\zeta) + \frac{1}{2}u(\zeta) - \frac{1}{2}u^3(\zeta) = 0, \tag{76}$$

whose exact solution derived by GKS is equation (28), which has the following initial conditions

$$u(0) = -\frac{1}{2}, u'(0) = -\frac{1}{4}. \tag{77}$$

The HWNS considers the solution of equation (76) in the form

$$u''(\zeta) = \sum_{i=1}^{2M} a_i h_i(\zeta). \tag{78}$$

By integrating equation (78) twice from $0 \to \zeta$ we obtain

$$\begin{aligned} u'(\zeta) &= \sum_{i=1}^{2M} a_i p_i(\zeta) + u'(0) \\ &= -\frac{1}{4} + \sum_{i=1}^{2M} a_i p_i(\zeta), \end{aligned} \tag{79}$$

$$\begin{aligned} u(\zeta) &= \sum_{i=1}^{2M} a_i Q_i(\zeta) - \frac{1}{4}\zeta + u(0) \\ &= -\frac{1}{2} - \frac{1}{4}\zeta + \sum_{i=1}^{2M} a_i Q_i(\zeta). \end{aligned} \tag{80}$$

By substituting from equations (78)–(80) into equation (76) we get

$$\begin{aligned} &\frac{1}{4}\sum_{i=1}^{2M} a_i h_i(\zeta) - \frac{3}{4}\left(-\frac{1}{4} + \sum_{i=1}^{2M} a_i P_i(\zeta)\right) \\ &\quad + \frac{1}{2}\left(-\frac{1}{2} - \frac{1}{4}\zeta + \sum_{i=1}^{2M} a_i Q_i(\zeta)\right) \\ &\quad - \frac{1}{2}\left(-\frac{1}{2} - \frac{1}{4}\zeta + \sum_{i=1}^{2M} a_i Q_i(\zeta)\right)^3 = 0. \end{aligned} \tag{81}$$

Satisfying equation (81) at the collocation points given in equation (57) we get

$$\begin{aligned} &\frac{1}{4}\sum_{i=1}^{2M} a_i h_i(\zeta_l) - \frac{3}{4}\left(-\frac{1}{4} + \sum_{i=1}^{2M} a_i P_i(\zeta_l)\right) \\ &\quad + \frac{1}{2}\left(-\frac{1}{2} - \frac{1}{4}\zeta_l + \sum_{i=1}^{2M} a_i Q_i(\zeta_l)\right) \\ &\quad - \frac{1}{2}\left(-\frac{1}{2} - \frac{1}{4}\zeta_l + \sum_{i=1}^{2M} a_i Q_i(\zeta_l)\right)^3 = 0\,,\ \ l = 1, 2, ...,2M. \end{aligned} \tag{82}$$

Let the parameter $J = 1 \to M = 2^J = 2 \to 2M = 4 \to l = 1, 2, 3, 4$ in equation (82)

$$\begin{aligned} &\frac{1}{4}\sum_{i=1}^{4} a_i h_i(\zeta_l) - \frac{3}{4}\left(-\frac{1}{4} + \sum_{i=1}^{4} a_i P_i(\zeta_l)\right) \\ &\quad + \frac{1}{2}\left(-\frac{1}{2} - \frac{1}{4}\zeta_l + \sum_{i=1}^{4} a_i Q_i(\zeta_l)\right) \\ &\quad - \frac{1}{2}\left(-\frac{1}{2} - \frac{1}{4}\zeta_l + \sum_{i=1}^{4} a_i Q_i(\zeta_l)\right)^3 = 0,\ l = 1, 2, 3, 4. \end{aligned} \tag{83}$$

Equation (83), at collocation points $\zeta_l = \dfrac{l - 0.5}{2M} = \dfrac{l - 0.5}{4}$, $l = 1, 2, 3, 4$, surrenders to a system of unknowns a_i, $i = 1, 2, 3, 4$, and its solution is

$$\begin{aligned} a_1 &= 0.0771199, \\ a_2 &= -0.0397252, \\ a_3 &= -0.0172571, \\ a_4 &= -0.0252802. \end{aligned} \tag{84}$$

Then, the Haar wavelet solution of equation (84) is

$$\begin{aligned} u(\zeta) &= -\frac{1}{2} - \frac{1}{4}\zeta + a_1 Q_1(\zeta) \\ &\quad + a_2 Q_2(\zeta) + a_3 Q_3(\zeta) + a_4 Q_4(\zeta) \\ &= -\frac{1}{2} - \frac{1}{4}\zeta 0.0771199 Q_1(\zeta) - 0.0397252 Q_2(\zeta) \\ &\quad - 0.0172571 Q_3(\zeta) - 0.0252802 Q_4(\zeta), \end{aligned} \tag{85}$$

$$Q\Psi(x, \tau) = u(\zeta) e^{i\eta(x,\tau)}$$

$$\begin{aligned} &\mathrm{Re}\,\Psi(x, \tau) = \\ &\begin{pmatrix} -\frac{1}{2} - \frac{1}{4}(x + \tau) + 0.0771199 Q_1(x + \tau) \\ -0.0397252 Q_2(x + \tau) \\ -0.0172571 Q_3(x + \tau) - 0.0252802 Q_4(x + \tau) \end{pmatrix} \\ &\quad \times \cos\left[-\frac{5}{4}x + \tau + 0.1\right], \end{aligned} \tag{86}$$

and

$$\begin{aligned} &\mathrm{Im}\Psi(x, \tau) = \\ &\begin{pmatrix} -\frac{1}{2} - \frac{1}{4}(x + \tau) + 0.0771199 Q_1(x + \tau) \\ -0.0397252 Q_2(x + \tau) \\ -0.0172571 Q_3(x + \tau) - 0.0252802 Q_4(x + \tau) \end{pmatrix} \\ &\times \sin\left[-\frac{5}{4}x + \tau + 0.1\right]. \end{aligned} \tag{87}$$

4.5. The numerical solution by the HWNS corresponding to the exact solution derived by the $\left(\frac{G'}{G}\right)$-expansion scheme (real part)

According to $\left(\dfrac{G'}{G}\right)$ the real part of equation (11) with the following values

$$\begin{aligned} &R = P = q = g_c = g_R = \gamma_R = n_R = w = k = 1, \\ &\delta = \frac{-10}{27},\ \gamma_c = \frac{2}{5}, \end{aligned} \tag{88}$$

becomes

$$\frac{1}{2}u'''(\zeta) - \frac{7}{18}u'(\zeta) - 3u'(\zeta)u^2(\zeta) - \frac{1}{9}u(\zeta) + u^3(\zeta) = 0, \tag{89}$$

whose exact solution derived by $\left(\dfrac{G'}{G}\right)$ is equation (40), which has the following initial conditions

$$u(0) = \frac{1}{6},\ u'(0) = -\frac{1}{12},\ u''(0) = \frac{1}{18}. \tag{90}$$

The Haar wavelet solution of equation (89) takes the form

$$u'''(\zeta) = \sum_{i=1}^{2M} a_i h_i(\zeta). \tag{91}$$

To reach $u(\zeta)$, we integrate equation (91) three times from

$0 \rightarrow \zeta$

$$u''(\zeta) = \sum_{i=1}^{2M} a_i p_i(\zeta) + u''(0) = \frac{1}{18} + \sum_{i=1}^{2M} a_i p_i(\zeta), \quad (92)$$

$$u'(\zeta) = \sum_{i=1}^{2M} a_i Q_i(\zeta) + \frac{1}{18}\zeta + u'(0) = -\frac{1}{12} + \frac{1}{18}\zeta + \sum_{i=1}^{2M} a_i Q_i(\zeta), \quad (93)$$

$$u(\zeta) = \sum_{i=1}^{2M} a_i R_i(\zeta) + \frac{1}{36}\zeta^2 - \frac{1}{12}\zeta + u(0) = \frac{1}{36}\zeta^2 - \frac{1}{12}\zeta + \frac{1}{6} + \sum_{i=1}^{2M} a_i R_i(\zeta). \quad (94)$$

Using equations (91)–(94) in equation (89) one can get

$$\frac{1}{2}\sum_{i=1}^{2M} a_i h_i(\zeta) - \frac{7}{18}\left(-\frac{1}{12} + \frac{1}{18}\zeta + \sum_{i=1}^{2M} a_i Q_i(\zeta)\right) - \frac{1}{9}\left(\frac{1}{36}\zeta^2 - \frac{1}{12}\zeta + \frac{1}{6} + \sum_{i=1}^{2M} a_i R_i(\zeta)\right) - 3\left(-\frac{1}{12} + \frac{1}{18}\zeta + \sum_{i=1}^{2M} a_i Q_i(\zeta)\right) \times \left(\frac{1}{36}\zeta^2 - \frac{1}{12}\zeta + \frac{1}{6} + \sum_{i=1}^{2M} a_i R_i(\zeta)\right)^2 + \left(\frac{1}{36}\zeta^2 - \frac{1}{12}\zeta + \frac{1}{6} + \sum_{i=1}^{2M} a_i R_i(\zeta)\right)^3 = 0\,. \quad (95)$$

Putting the level of resolution $J = 1 \rightarrow M = 2^J = 2 \rightarrow 2M = 4 \rightarrow l = 1, 2, 3, 4$, satisfying equation (95) at the collocation points $\zeta_l = \frac{l - 0.5}{2M} = \frac{l - 0.5}{4}$, $l = 1, 2, 3, 4$, we obtain a system in the unknowns a_i, $i = 1, 2, 3, 4$, and by solving this system we find

$$\begin{aligned} a_1 &= -0.0250399, \\ a_2 &= -0.0067265, \\ a_3 &= -0.00423359, \\ a_4 &= -0.00253455. \end{aligned} \quad (96)$$

The Haar wavelet solution of equation (89) is

$$u(\zeta) = \frac{1}{36}\zeta^2 - \frac{1}{12}\zeta + \frac{1}{6} + a_1 R_1(\zeta) + a_2 R_2(\zeta) + a_3 R_3(\zeta) + a_4 R_4(\zeta) = \frac{1}{36}\zeta^2 - \frac{1}{12}\zeta + \frac{1}{6} - 0.0250399\, R_1(\zeta) - 0.0067265\, R_2(\zeta) - 0.00423359 R_3(\zeta) - 0.00253455\, R_4(\zeta). \quad (97)$$

And hence, $\Psi(x, \tau) = u(\zeta)e^{i\eta(x,\tau)}$, from which we get

$$\mathrm{Re}\,\Psi(x, \tau) = \begin{pmatrix} \frac{1}{36}(x+\tau)^2 + \frac{1}{6} - 0.0250399\, R_1(x+\tau) \\ -0.0067265\, R_2(x+\tau) - 0.0042336 R_3(x+\tau) \\ -0.00253455\, R_4(x+\tau) - \frac{1}{12}(x+\tau) \end{pmatrix} \times \cos\left[x - \frac{10}{27}\tau + 0.1\right], \quad (98)$$

$$\mathrm{Im}\Psi(x, \tau) = \begin{pmatrix} \frac{1}{36}(x+\tau)^2 + \frac{1}{6} - 0.0250399\, R_1(x+\tau) \\ -0.0067265\, R_2(x+\tau) - 0.00423359 R_3(x+\tau) \\ -0.00253455\, R_4(x+\tau) - \frac{1}{12}(x+\tau) \end{pmatrix} \times \sin\left[x - \frac{10}{27}\tau + 0.1\right]. \quad (99)$$

4.6. The numerical solution by the HWNS corresponding to the exact solution derived by the $\left(\frac{G'}{G}\right)$-expansion scheme (imaginary part)

The imaginary part equation (12) with the following

$$\delta = R = g_R = \gamma_c = \gamma_R = n_R = w = k = P = q = 1, \quad g_c = \frac{11}{2}, \quad (100)$$

is reduced to

$$\frac{5}{2}u''(\zeta) - \frac{5}{2}u(\zeta) - 5u^3(\zeta) = 0, \quad (101)$$

whose exact solution derived by $\left(\frac{G'}{G}\right)$ is equation (47), which has the following initial conditions

$$u(0) = i\sqrt{2}\,,\ u'(0) = 0. \quad (102)$$

The HWNS considers the solution of equation (101) in the form

$$u''(\zeta) = \sum_{i=1}^{2M} a_i h_i(\zeta). \quad (103)$$

By integrating equation (103) twice from $0 \rightarrow \zeta$ to obtain $u(\zeta)$

$$u'(\zeta) = \sum_{i=1}^{2M} a_i p_i(\zeta) + u'(0) = \sum_{i=1}^{2M} a_i p_i(\zeta), \quad (104)$$

$$u(\zeta) = \sum_{i=1}^{2M} a_i Q_i(\zeta) + u(0) = i\sqrt{2} + \sum_{i=1}^{2M} a_i Q_i(\zeta). \quad (105)$$

Inserting equations (103)–(105) into equation (101) we get

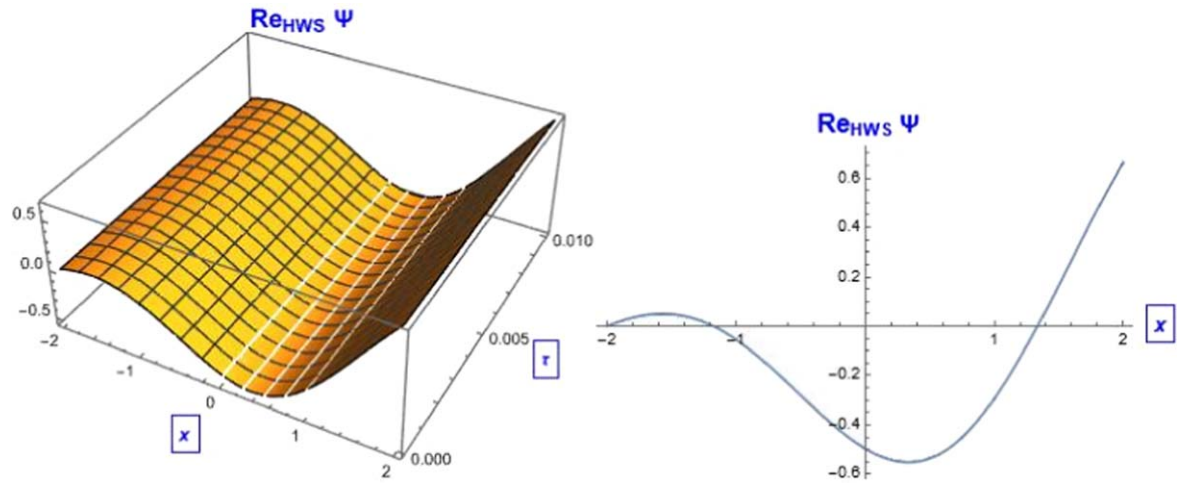

Figure 16. The numerical solution behavior to equation (86) with values given in equation (75).

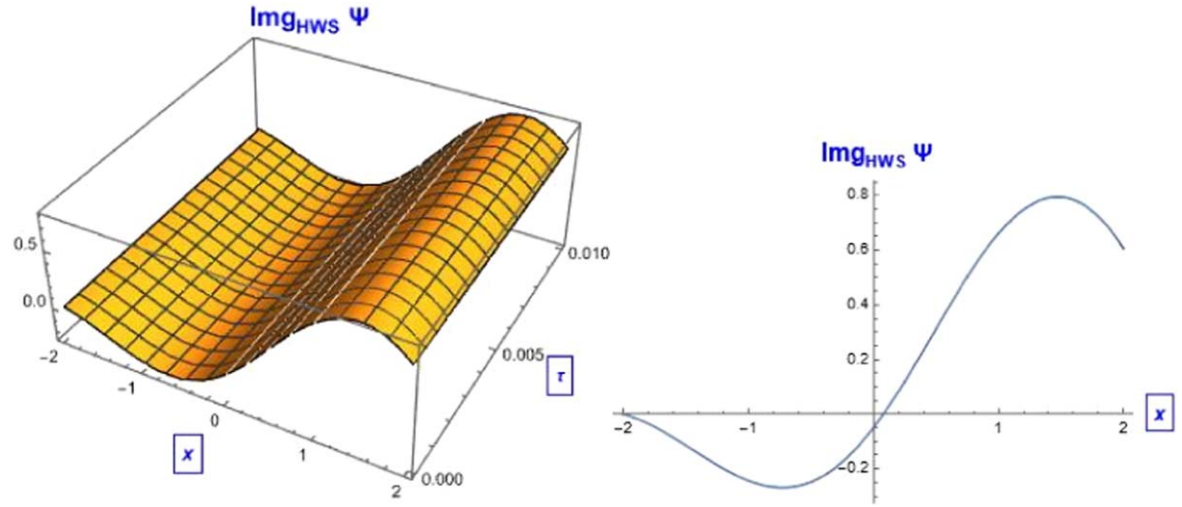

Figure 17. The numerical solution behavior to equation (87) with values given in equation (75).

$$\frac{5}{2}\sum_{i=1}^{2M} a_i h_i(\zeta) - \frac{5}{2}\left(i\sqrt{2} + \sum_{i=1}^{2M} a_i Q_i(\zeta)\right) - 5\left(\mathrm{i}\sqrt{2} + \sum_{i=1}^{2M} a_i Q_i(\zeta)\right)^3 = 0. \tag{106}$$

Taking the level of resolution $J = 1$, satisfying equation (106) at the collocation points $\zeta_l = \dfrac{l-0.5}{2M} = \dfrac{l-0.5}{4}$, $l = 1, 2, 3, 4$, a system in the unknowns a_i, $i = 1, 2, 3, 4$ is obtained. Solving this system, we get

$$\begin{aligned} a_1 &= 0.175656\mathrm{i}, \\ a_2 &= -2.84584\mathrm{i}, \\ a_3 &= -1.23671\mathrm{i}, \\ a_4 &= -1.074\mathrm{i}. \end{aligned} \tag{107}$$

Then the Haar wavelet solution of equation (110) is:

$$u(\zeta) = \mathrm{i}\sqrt{2} + 0.175656\mathrm{i}Q_1[\zeta] - 2.84584\mathrm{i}Q_2[\zeta] - 1.23671\mathrm{i}Q_3[\zeta] - 1.074\mathrm{i}Q_4[\zeta]. \tag{108}$$

And hence, $\Psi(x, \tau) = u(\zeta)\mathrm{e}^{\mathrm{i}\eta(x,\tau)}$, from which we get

$$\mathrm{Re}\,\Psi(x, \tau) = -\begin{pmatrix} \sqrt{2} + 0.175656Q_1[x+\tau] - 2.84584Q_2[x+\tau] \\ -1.23671Q_3[x+\tau] - 1.074Q_4[x+\tau] \end{pmatrix} \times \sin[x + \tau + 0.1], \tag{109}$$

$$\mathrm{Im}\Psi(x, \tau) = \begin{pmatrix} \sqrt{2} + 0.175656Q_1[x+\tau] - 2.84584Q_2[x+\tau] \\ -1.23671Q_3[x+\tau] - 1.074Q_4[x+\tau] \end{pmatrix} \times \cos[x + \tau + 0.1]. \tag{110}$$

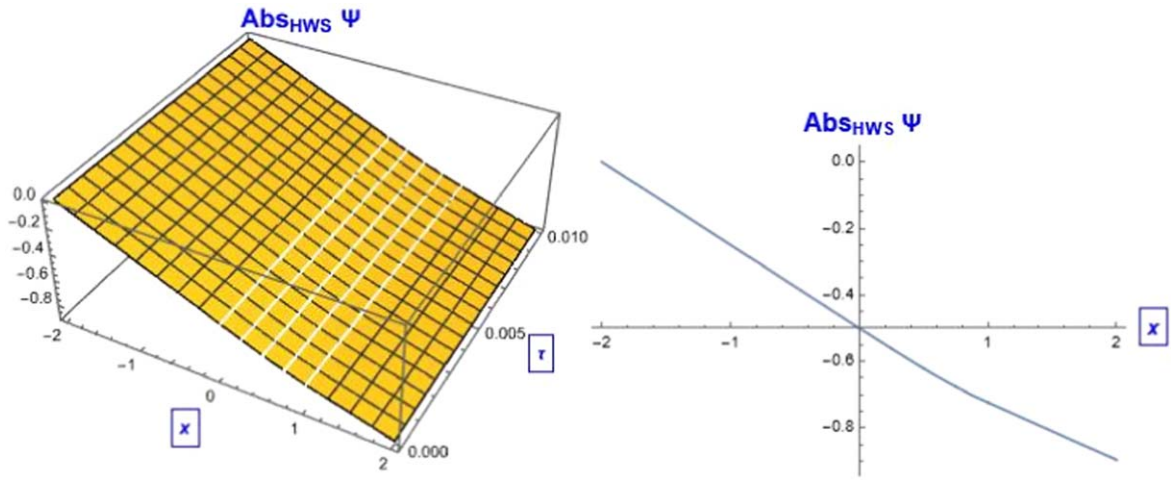

Figure 18. The 2D and 3D soliton HWN solution behavior of $|\Psi|$ equations (86) or (87).

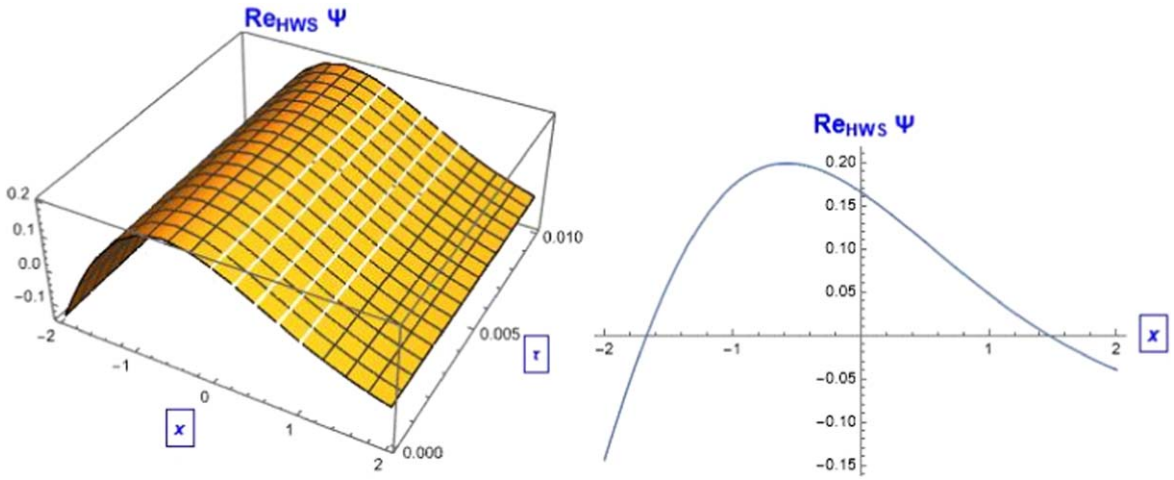

Figure 19. The numerical solution behavior to the Re. part of equation (98) with values $R = P = q = g_c = g_R = \gamma_R = n_R = w = k = 1$, $\delta = \dfrac{-10}{27}$, $\gamma_c = \dfrac{2}{5}$.

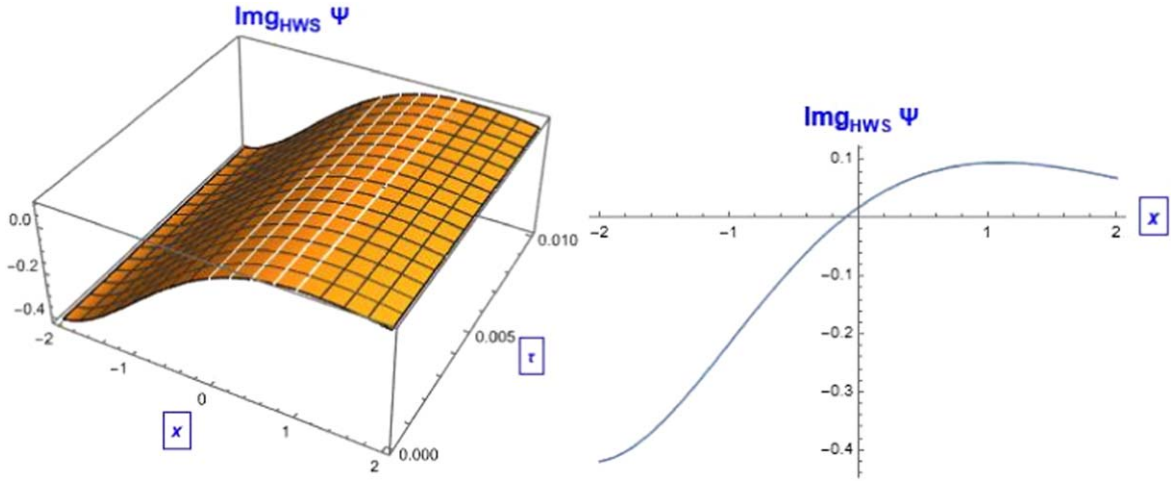

Figure 20. The numerical solution behavior to the Im. part of equation (99) with values $R = P = q = g_c = g_R = \gamma_R = n_R = w = k = 1$, $\delta = \dfrac{-10}{27}$, $\gamma_c = \dfrac{2}{5}$.

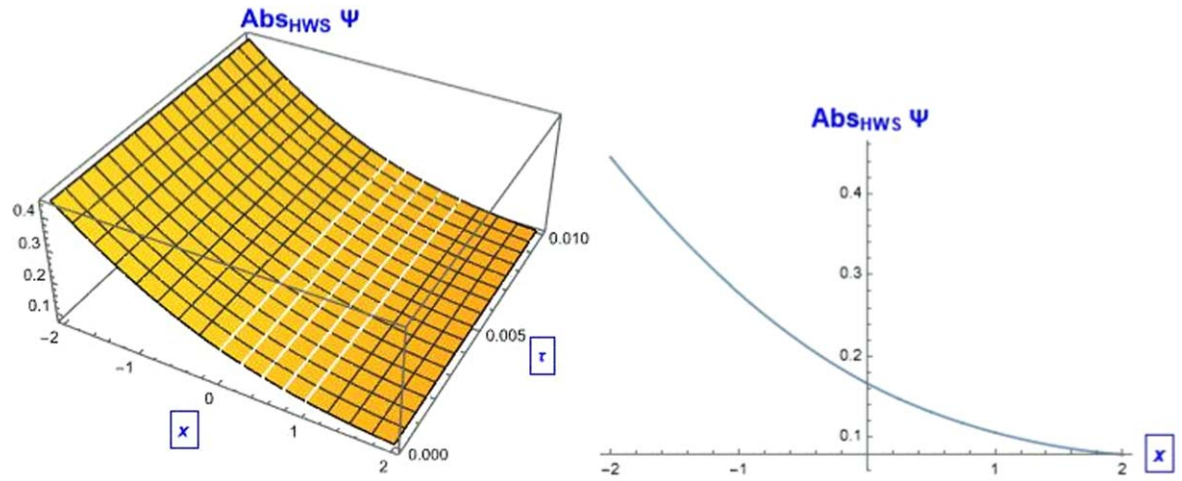

Figure 21. The 2D and 3D soliton HWN solution behavior of $|\Psi|$ equation (98) or (99).

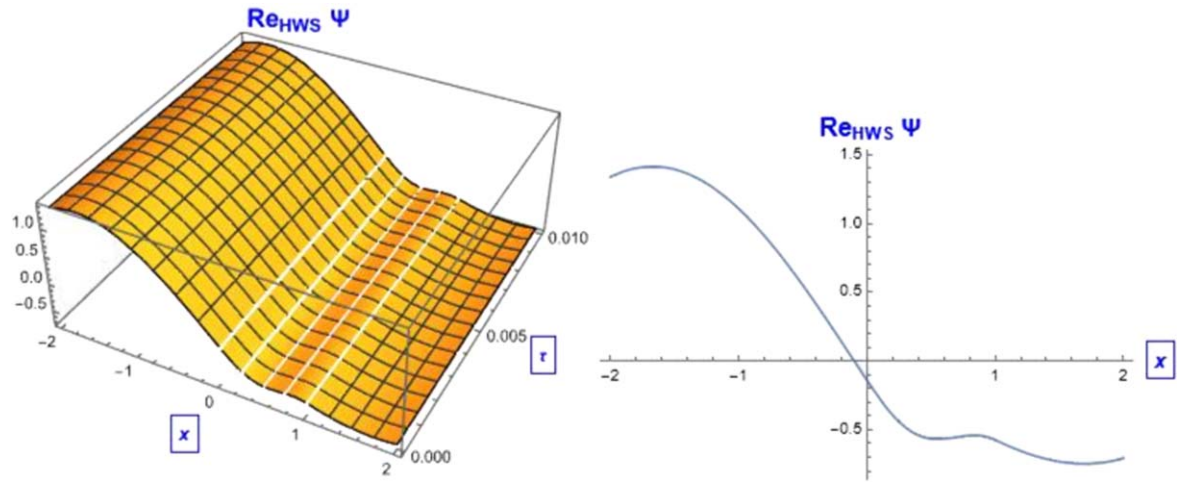

Figure 22. The numerical solution behavior to the Re. part of equation (109) with values $\delta = R = g_R = \gamma_c = \gamma_R = n_R = w = k = P = q = 1$, $g_c = \dfrac{11}{2}$.

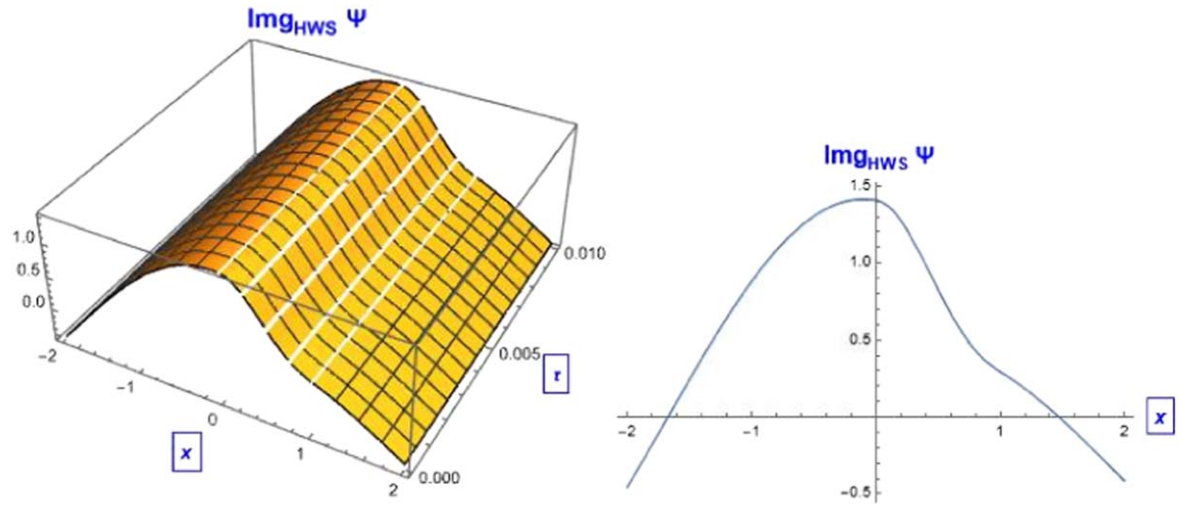

Figure 23. The numerical solution behavior to the Im. part of equation (110) with values $\delta = R = g_R = \gamma_c = \gamma_R = n_R = w = k = P = q = 1$, $g_c = \dfrac{11}{2}$.

5. Conclusion

In this paper, we succeeded in deriving diverse enormous soliton solutions to the Gross–Pitaevskii equation, which describes the dynamics of two dark solitons in a polarization condensate under non-resonant pumping, analytically for the first time using the generalized Kudryashov method and the (G'/G)-method. The extracted solutions in the framework of these two suggested schemes appear in forms that include dark, bright, combined bright-shaped and dark-shaped soliton solutions, hyperbolic function soliton solutions, singular shaped soliton solutions and other rational soliton solutions. Moreover, the Haar wavelet numerical method, which is one of the famous techniques in numerical methods, has been utilized to explore the numerical solutions for all realized soliton solutions by the above two techniques. The 2D and 3D graphs have been designed utilizing the Mathematica program and the figures simulations have been configured to show the agreement range between the soliton solutions and the numerical solutions, which corresponded perfectly in figures [1–23]. Our results are new compared with [22] who used the variational approach and analytically derived the time evolution equations for the soliton parameters and presented the first analytical result on the two-dark soliton problem in the context of a polarization Bose–Einstein Condensates formed under non-resonant pumping by solving the dissipative Gross–Pitaevskii equation that compares this analytical result with the numerical solutions for the trajectory of two solitons directly obtained from the dissipative Gross–Pitaevskii equation. Our realized analytical solutions and their corresponding numerical solutions have not been achieved before.

References

[1] Pethick C J and Smith H 2008 *Bose–Einstein Condensation in Dilute Gases* (Cambridge University Press)

[2] Kevrekidis P G, Frantzeskakis D J and Carretero-Gonzalez R 2015 *The Defocusing Nonlinear Schrödinger Equation: From Dark Solitons to Vortices and Vortex Rings* (Philadelphia, PA: SIAM)

[3] Kevrekidis P and Frantzeskakis D 2016 Solitons in coupled nonlinear Schrödinger models: a survey of recent developments *Rev. Phys.* **1** 140–53

[4] Xu X, Chen L, Zhang Z and Liang Z 2019 Dark–bright solitons in spinor polarisation condensates under nonresonant pumping *J. Phys.* B **52** 025303

[5] Zhou Q 2022 Influence of parameters of optical fibers on optical soliton interactions *Chin. Phys. Lett.* **39** 010501

[6] Bobrovska N, Ostrovskaya E A and Matuszewski M 2014 Stability and spatial coherence of nonresonantly pumped exciton-polariton condensates *Phys. Rev.* B **90** 205304

[7] Keeling J, Marchetti F M, Szymańska M H and Littlewood P B 2007 Collective coherence in planar semiconductor microcavities *Semicond. Sci. Technol.* **22** R1

[8] Luders C, Pukrop M, Rozas E, Schneider C, Höfling S, Sperling J, Schumacher S and Amann M 2021 Quantifying quantum coherence in polarisation condensates *PRX Quantum* **2** 030320

[9] Schneider C, Winkler K, Fraser M D, Kamp M, Yamamoto Y, Ostrovskaya E A and Hofling S 2016 Exciton-polarisation trapping and potential landscape engineering *Rep. Prog. Phys.* **80** 016503

[10] Wang B, Zhang Z and Li B 2020 Soliton molecules and some hybrid solutions for the nonlinear Schrödinger equation *Chin. Phys. Lett.* **37** 030501

[11] Zhao L C, Qin Y H, Wang W L and Yang Z Y 2020 A direct derivation of the dark soliton excitation energy *Chin. Phys. Lett.* **37** 050502

[12] Zhang K, Wen W, Lin J and Li H J 2021 Generation and stability of diversiform nonlinear localized modes in exciton–polarisation condensates; *New J. Phys.* **23** 033011

[13] Cheng S C and Chen T W 2020 Topological spin-Meissner states in nonequilibrium polarisation condensates *Phys. Rev.* B **101** 125304

[14] Mu N M A, Rubo Y G and Toikka L A 2020 Long Josephson junctions with exciton-polarisation condensates *Phys. Rev.* B **101** 184509

[15] Jiang Y, Wang G, Sun X M, Feng S H and Xue Y 2019 Manipulation of a stable dark soliton train in polarisation condensate *Opt. Express* **27** 10185

[16] Opala A, Pieczarka M, Bobrovska N and Matuszewski M 2018 Dynamics of defect-induced dark solitons in an exciton-polarisation condensate *Phys. Rev.* B **97** 155304

[17] Stepanov P, Amelio I, Rousset J G, Bloch J, Lemaitre A, Amo A, Minguzzi A, Carusotto I and Richard M 2019 Dispersion relation of the collective excitations in a resonantly driven polarisation fluid *Nat. Commun.* **10** 3869

[18] Maıtre A, Lerario G, Medeiros A, Claude F, Glorieux Q, Giacobino E, Pigeon S and Bramati A 2020 Dark-soliton molecules in an exciton-polarisation superfluid *Phys. Rev. X* **10** 041028

[19] Lerario G, Koniakhin S V, Maître A, Solnyshkov D, Zilio A, Glorieux Q, Malpuech G, Giacobino E, Pigeon S and Bramati A 2020 Parallel dark-soliton pair in a bistable two-dimensional exciton-polarisation superfluid *Phys. Rev. Res.* **2** 042041

[20] Claude F *et al* 2020 Taming the snake instabilities in a polarisation superfluid *Optica* **7** 1660

[21] Yulin A V, Skryabin D V and Gorbach A V 2015 Dark solitons and vortices in the intrinsic bistability regime in exciton polarisation condensates *Phys. Rev.* B **92** 064306

[22] Zhang Y, Jia C and Liang Z 2022 Dynamics of two dark solitons in a polarisation condensate *Chin. Phys. Lett.* **39** 020501

[23] Kasprzak J *et al* 2006 Bose–Einstein condensation of exciton polarisations *Nature* **443** 409

[24] Deng H, Haug H and Yamamoto Y 2010 Exciton-polarisation Bose–Einstein condensation *Rev. Mod. Phys.* **82** 1489

[25] Carusotto I and Ciuti C 2013 Quantum fluids of light *Rev. Mod. Phys.* **85** 299

[26] Keeling J and Berloff N G 2011 Exciton–polarisation condensation *Contemp. Phys.* **52** 131

[27] Tariq, K U, Wazwaz A M and Javed R 2022 Construction of different wave structures, stability analysis and modulation instability of the coupled nonlinear Drinfel'd–Sokolov–Wilson model *Chaos, Solitons Fractals* **166** 112903

[28] Tariq, K U, Bekir A and Sana Nisar S 2023 The dynamical structures of the Sharma-Tasso-Olver model in doubly dispersive medium *Chaos, Solitons Fractals* **177** 114290

[29] Badshah F, Tariq K U, Bekir A, Tufail R N and Ilyas H 2024 Lump, periodic, travelling, semi-analytical solutions and stability analysis for the Ito integro-differential equation arising in shallow water waves *Chaos, Solitons Fractals* **182** 114783

[30] Badshah, F, Tariq K U, Ilyas H and Tufail R N 2024 Soliton, lumps, stability analysis and modulation instability for an extended (2+1)-dimensional Boussinesq model in shallow water *Chaos, Solitons Fractals* **187** 115352

[31] Ay N G and Yaşar E 2023 The residual symmetry, Bäcklund transformations, CRE integrability, and interaction

solutions: (2+1)-dimensional Chaffee–Infante equation *Commun. Theor. Phys.* **75** 115004
[32] Wertz E *et al* 2010 Spontaneous formation and optical manipulation of extended polarisation condensates *Nat. Phys.* **6** 860
[33] Smirnov L A, Smirnova D A, Ostrovskaya E A and Kivshar Y S 2014 Dynamics and stability of dark solitons in exciton-polarisation condensates *Phys. Rev.* B **89** 235310
[34] Akbar M A, Wazwaz A M, Mahmud F, Baleanu D, Roy R, Barman H K, Mahmoud W, Al Sharifi M A A and Osman M S 2022 Dynamical behavior of solitons of the perturbed nonlinear Schrödinger equation and microtubules through the generalized Kudryashov scheme *Res. Phys.* **43** 106079
[35] Zahran E H M, Bekir A, Ibrahim R A and Myrzakulove R 2024 The new soliton solution types to the Myrzakulov–Lakshmanan-XXXII-equation *AIMS Mathematics* **9** 6145–60
[36] Genc G, Ekici M, Biswas A and Belic M R 2020 Cubic-quartic optical solitons with Kudryashov's law of refractive index by F-expansions schemes *Res. Phys.* **18** 103273
[37] Kumar D, Seadawy A R and Joardar A K 2018 Modified Kudryashov method via new exact solutions for some conformable fractional differential equations arising in mathematical biology *Chin. J. Phys.* **56** 75–85
[38] Bekir A 2008 Application of the (G'/G)-expansion method for nonlinear evolution equations *Phys. Lett.* A **372** 3400–6
[39] Zahran E H M, Bekir A and Ibrahim R A 2024 Effective analytical solutions versus numerical treatments of Chavy–Waddy–Kolokolnikov bacterial aggregates model in phototaxic *Eur. Phys. J. Plus* **139** 135
[40] Zahran E H M and Bekir A 2023 Unexpected configurations for the optical solitons propagation in lossy fiber system with dispersion terms effect *Math. Meth. Appl. Sci.* **46** 4055–69
[41] Chen C F and Hsiao C H 1997 Haar wavelet method for solving lumped and distributed parameter systems *IEEE Proceeding Control Theory Appl.* **144** 87–94
[42] Lepik U 2008 Application of Haar wavelet transform to solving integral and differential equations *Appl. Math. Comput.* **57** 28–46
[43] Zahran E H M, Bekir A and Ibrahim R A 2024 Unique soliton solutions to the nonlinear Schrödinger equation with weak non-locality and cubic–quintic–septic nonlinearity in nonlinear optical fibers *Appl. Phys.* B **130** 34
[44] Lepik U and Hein H 2014 *Haar Wavelet with Applications* (Springer)
[45] Youssef I K and Ibrahim R A 2017 On the performance of Haar wavelet approach for boundary value problems and systems of Fredholm integral equations *Math. Comput. Sci.* **2** 39–46